

AD-A034 193

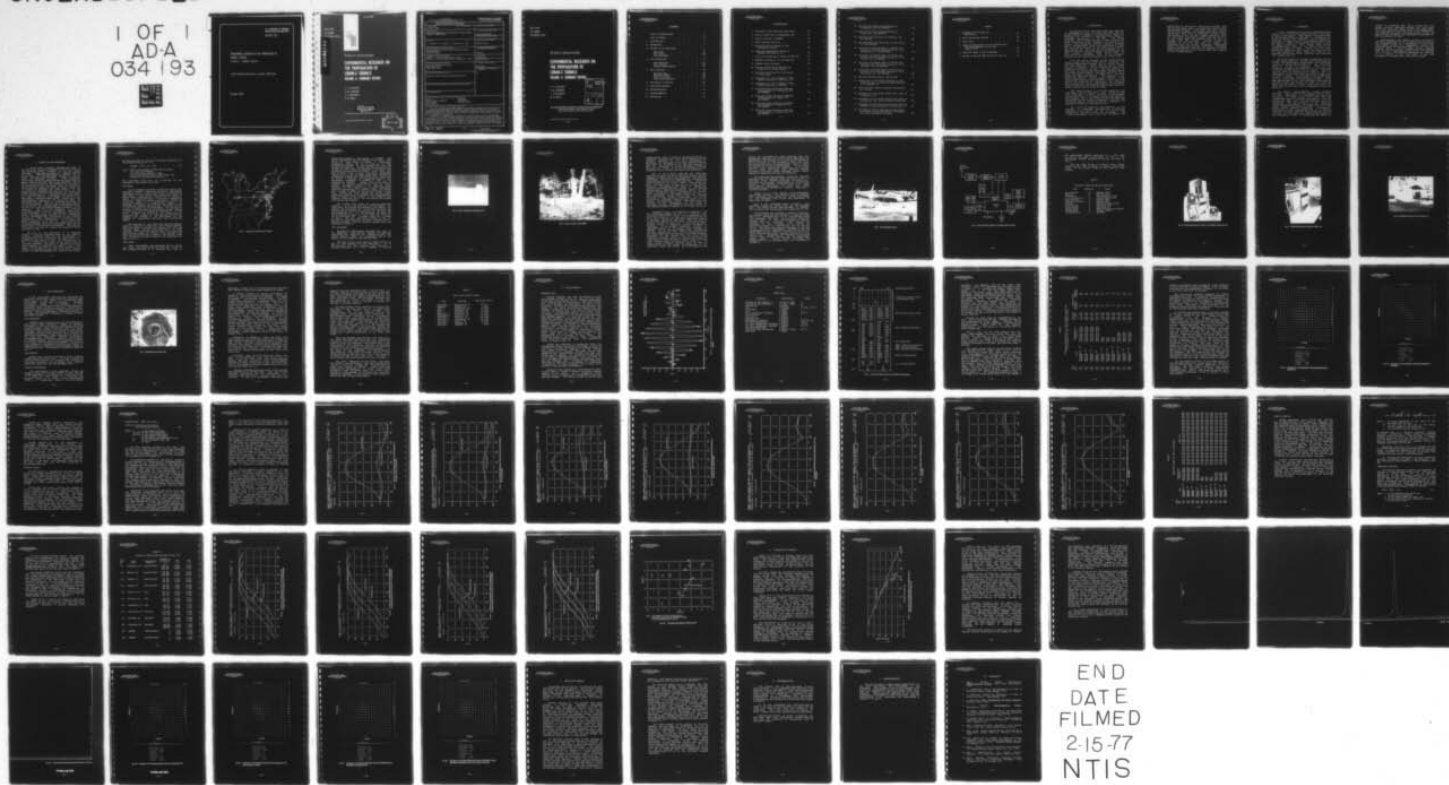
JOHNS HOPKINS UNIV LAUREL MD APPLIED PHYSICS LAB  
EXPERIMENTAL RESEARCH ON THE PROPAGATION OF LORAN-C SIGNALS. VO--ETC(U)  
OCT 76 L F FEHLNER, T W JERARDI, T A MCCARTY N00017-72-C-4401  
APL/JHU-TG-1298A

F/G 17/7

UNCLASSIFIED

NL

1 OF 1  
AD-A  
034 193



END  
DATE  
FILMED  
2-15-77  
NTIS

U.S. DEPARTMENT OF COMMERCE  
National Technical Information Service

AD-A034 193

EXPERIMENTAL RESEARCH ON THE PROPAGATION OF  
LORAN-C SIGNALS

VOLUME A. SUMMARY REPORT

JOHNS HOPKINS UNIVERSITY, LAUREL, MARYLAND

OCTOBER 1976

DC

012009

APL/JHU  
TG 1298A  
OCTOBER 1976



ADA U34193

*Technical Memorandum*

**EXPERIMENTAL RESEARCH ON  
THE PROPAGATION OF  
LORAN-C SIGNALS  
VOLUME A: SUMMARY REPORT**

L. F. FEHLNER  
T. W. JERARDI  
T. A. McCARTY  
R. G. ROLL

REPRODUCED BY  
**NATIONAL TECHNICAL  
INFORMATION SERVICE**  
U. S. DEPARTMENT OF COMMERCE  
SPRINGFIELD, VA. 22161

THE JOHNS HOPKINS UNIVERSITY ■ APPLIED PHYSICS LABORATORY

Approved for public release; distribution unlimited.

DDC  
RECORDED  
JAN 11 1977  
B



APL/JHU  
TG 1298A  
OCTOBER 1976

*Technical Memorandum*

**EXPERIMENTAL RESEARCH ON  
THE PROPAGATION OF  
LORAN-C SIGNALS  
VOLUME A: SUMMARY REPORT**

L. F. FEHLNER  
T. W. JERARDI  
T. A. McCARTY  
R. G. ROLL

ACCESSION for	
NTIS	White Section <input checked="" type="checkbox"/>
DTIC	Buff Section <input type="checkbox"/>
UNCLASSIFIED	<input type="checkbox"/>
JUSTIFICATION	
BY	
DISTRIBUTION AVAILABILITY CODES	
DISL.	AVAIL. and/or SPECIAL
A	

THE JOHNS HOPKINS UNIVERSITY ■ APPLIED PHYSICS LABORATORY  
Johns Hopkins Road, Laurel, Maryland 20810  
Operating under Contract N00017-72-C-4401 with the Department of the Navy

Approved for public release; distribution unlimited.

CONTENTS

List of Illustrations . . . . .	4
List of Tables . . . . .	6
1. Introduction . . . . .	7
2. Background . . . . .	9
3. Design of the Experiment . . . . .	11
Ray Paths . . . . .	12
Test Sites . . . . .	12
Test Equipment . . . . .	14
4. Test Operations . . . . .	25
Site Selection . . . . .	25
Site Surveys . . . . .	25
Loran-C Measurements . . . . .	25
5. Data Analysis . . . . .	30
Recorded Data . . . . .	30
Observed Signal . . . . .	39
Time of Arrival . . . . .	51
Correction Function . . . . .	52
6. Discussion of Results . . . . .	60
7. Concluding Remarks . . . . .	71
8. Recommendations . . . . .	72
9. Acknowledgments . . . . .	74
10. References . . . . .	75

ILLUSTRATIONS

1	Locations of Ray Paths and Test Sites . . .	13
2	View of Field Site at Georgetown, DE . . .	15
3	Loran-C Antenna at NAVOBSY . . . . .	16
4	Piper Cherokee Aircraft . . . . .	19
5	Functional Block Diagram of the Measurement System . . . . .	20
6	Fixed Site Measurement System in NAVOBSY Building No. 54 . . . . .	22
7	Field Site Measurement System in USAF Van . . .	23
8	NAVOBSY Building No. 54 and USAF Van . . . .	24
9	NAVOBSY Survey Monument . . . . .	26
10	Typical Loran-C Pulse Showing the Location of Voltage Samples . . . . .	31
11	Raw Data Tape Format for Each Block of Recording . . . . .	33
12	Histogram of I and Q Samples of Dana Signals Observed at Danville, IN . . . . .	37
13	Histogram of I and Q Samples of Dana Signals Observed at NAVOBSY . . . . .	38
14	Sine and Cosine Modulation Observed Simultaneously at Wilmington, NC, and NAVOBSY . . . . .	42
15	Sine and Cosine Modulation Observed Simultaneously at Dexter, NY, and NAVOBSY . . . . .	43
16	Sine and Cosine Modulation Observed Simultaneously at Danville, IN, and NAVOBSY . . . . .	44
17	Sine and Cosine Modulation Observed Simultaneously at Toms River, NJ, and NAVOBSY . . . . .	45

18	The Carolina Beach Pulse Envelope at Wilmington, NC, and NAVOBSY . . . . .	46
19	The Carolina Beach Pulse Envelope at Dexter, NY, and NAVOBSY . . . . .	47
20	The Dana Pulse Envelope at Danville, IN, and NAVOBSY . . . . .	48
21	The Nantucket Pulse Envelope at Toms River, NJ, and NAVOBSY . . . . .	49
22	Locations of Leading Edges of Pulses with Standard Zero Crossings Aligned at 30 $\mu$ s, Wilmington, NC, and NAVOBSY . . . . .	55
23	Locations of Leading Edges of Pulses with Standard Zero Crossings Aligned at 30 $\mu$ s, Dexter, NY, and NAVOBSY . . . . .	56
24	Locations of Leading Edges of Pulses with Standard Zero Crossings Aligned at 30 $\mu$ s, Danville, IN, and NAVOBSY . . . . .	57
25	Locations of Leading Edges of Pulses with Standard Zero Crossings Aligned at 30 $\mu$ s, Toms River, NJ, and NAVOBSY . . . . .	58
26	The Relationship Between SPM and ECM . . . . .	59
27	Attenuation of the Signal Relative to the Field Strength of Carolina Beach Observed at Wilmington, NC . . . . .	61
28	Power Spectral Density Showing Interference at 179 kHz . . . . .	65
29	Histogram of First-Stage Edited Data Taken at Georgetown, DE . . . . .	67
30	Histogram of First-Stage Edited Data Taken at Georgetown, DE, after Frequency Filtering . . . . .	68
31	Histogram of First-Stage Edited Data Taken at NAVOBSY During Recording at Georgetown, DE . . . . .	69
32	Histogram of First-Stage Edited Data Taken at NAVOBSY During Recording at Georgetown, DE, after Frequency Filtering . . . . .	70

TABLES

1	Equipment Used During the Experiment . . . . .	21
2	Test Field Sites Visited . . . . .	29
3	Taped Data . . . . .	32
4	Signal-to-Noise Ratio of the Primary Data from Measurements at the 12th Sample Point . . . . .	35
5	Observed Times of Zero Crossings . . . . .	50
6	Values of SPM and ECM Plotted in Fig. 26 . . . . .	54

## 1. INTRODUCTION

The Applied Physics Laboratory (APL) has conducted an experiment for the U.S. Air Force (USAF) and the Defense Advanced Research Projects Agency (DARPA) to determine the validity of one facet of the theory of groundwave propagation at 100 kHz. The theory indicates that if proper account is taken of group and phase velocities in the propagation of pulses of the Loran-C radio navigation service, geodetic position should be computable using the vacuum speed of light and the times of arrival of the pulse and the carrier. Specifically, the test goal was to determine if an analytic function can be developed for operational use that relates secondary phase factor (SPF) to envelope-to-cycle difference (ECD) so that geodetic position can be computed accurately and in real time.

Test data were obtained in the eastern United States using the East Coast Loran-C chain and two identical measurement systems, one in a mobile test van and the other at a fixed site at the U.S. Naval Observatory (NAVOBSY). The van occupied 10 field sites during the course of the test. APL was assisted in this test by NAVOBSY and the Defense Mapping Agency Topographic Center (DMATC). The positions of all sites were precisely surveyed by DMATC using the Navy Navigation Satellite System. The sites are on ray paths from Loran-C stations through NAVOBSY. A team from NAVOBSY executed time transfers to each field site during the collection of loran data. The collected data include very accurate measurements of the Loran-C signal voltage and the absolute time at which they were made at each of the 10 pairs of sites.

This report (Volume A of TG 1298) summarizes the experiment and the findings to date. Volume B covers test operations, Volume C describes the measurement system, and Volume D documents the data, the analysis, and findings. All of the volumes are written under the assumption that the reader is reasonably familiar with the Loran-C system of radionavigation. Reference 1 is suggested reading for those who are not.

As a result of extensive data analysis, it was possible to establish statistically significant measures of SPF and ECD for each of the 12 tests conducted at the field sites and at NAVOBSY. The voltage measurements were used also to isolate the

modulations of the carrier that give the pulses from the Carolina Beach, Dana, and Nantucket Stations their unique characteristics. The pulses from each station contain both in-phase and in-quadrature modulations of the carrier that make it impossible to make direct observations of the carrier. Largely because of this, the functional relationship between ECD and SPF that, it was hoped, would be derived from the data is presently not well defined. However, trends are observed in the data that tend to support the hypothesis that the desired functional relationship exists, at least under certain conditions. Additional analysis and perhaps tests will be necessary to define these conditions or to prove conclusively the existence of such a relationship.

## 2. BACKGROUND

In 1914, Sommerfeld and Brillouin published papers (Refs. 2 and 3) that have become classics in the field of signal propagation. These papers were republished by the Academic Press in 1960 (Ref. 4). Sommerfeld and Brillouin proved that Einstein's famous theoretical postulate, "a signal cannot be transmitted faster than the speed of light," is consistent with observed group and phase velocities, even though under certain circumstances the group or the phase velocity may exceed the speed of light. Since 1914, the basic mathematics associated with group and phase velocity has been explored at great length, and many of the important results have found their way into textbooks (for example, Ref. 5).

The Triad satellite, launched in September 1972 as an experimental member of the Navy Navigation Satellite System, had phase-coded, pseudorandom noise-modulated carriers at 150 and 400 MHz (Ref. 6). By a fortuitous quirk of nature, the dispersive effect of the ionosphere on signals that penetrate it at frequencies of 150 and 400 MHz turns out to be useful. The phase velocity, which is greater than the speed of light, is compensated by the group velocity, which is less than the speed of light. To first order, this compensation is exact. Therefore, the average of group and phase velocity can be taken to be the speed of light. It has been demonstrated in the Triad experiment that geodetic position fixes that account for both the group and phase velocity using a single, modulated carrier are essentially free of error due to ionospheric refraction (Ref. 7).

The Loran-C radionavigation system transmits precisely timed pulses in the frequency band of 90 to 110 kHz. Many years of experience with groundwave propagation of these pulses have shown that the transmission times of the group and phase to a receiver are not the same. They vary with distance from the transmitter and are functions of the electrical properties of the medium. The electrical properties exhibit substantial spatial variations and, to a much lesser extent, temporal variations. Consequently, predictions of the transmission time to a specific location, of either group or phase alone, are not very accurate. On the other hand, numerous observations of the transmission times of both group and phase at a

variety of locations lead one to suspect that the medium produces dispersive effects and that these effects on group and phase velocity are compensating. If we only knew the functional form of the compensation and measured both group and phase arrival times, we might be able to deduce the transmission times based on the vacuum speed of light.

Unfortunately, the medium in which the Loran-C groundwave propagates is not as easily characterized as the ionosphere, and, as a consequence, the functional relationship between the transmission times of the group and phase is not well known. It was therefore proposed during a Loran Interservice Group meeting (Ref. 8) that an experiment should be run to determine this function. The proposed experiment was initiated at the request of the USAF (Ref. 9) and was subsequently co-sponsored by the USAF and DARPA.

### 3. DESIGN OF THE EXPERIMENT

A typical loran receiver measures the times of arrival of the last zero crossing of the third cycle in the received pulses, relative to its own timing reference. These arrival times are commonly referred to as TOA's. The TOA measurement is made on all the pulses received from the master station and from at least two secondary stations. Time difference coordinates (TD's) are then produced by subtracting the master station TOA from each of the secondary station TOA's. Typical receivers also measure the position of the pulse relative to the phase. This measurement is usually made by adding to the loran pulse a pulse that is formed by delaying the loran pulse 5  $\mu$ s and adjusting its amplitude such that the sum of the two pulses produces a null at the location of a "tag" point on the leading edge of a "standard" loran pulse shape. The time of this null with respect to the TOA is a measurement parameter known as ECD. Adding ECD to TOA then produces a measure of the pulse TOA under the assumption that the pulse, as received, qualifies as the standard shape. ECD is used to determine whether or not the TOA is being measured on the desired cycle. The TD's are used to compute geodetic position of the receiver. The TD's are converted to distance differences using an average propagation speed of the loran groundwave. Two or more distance differences permit the simultaneous solution for the intersection of the hyperbolas that are defined by the distance differences. This intersection is an estimate of the geodetic position of the receiver. It is associated with a systematic error that is proportional to the difference between the actual propagation speed and the speed used in the distance calculation. The additive factors that are used to correct the systematic errors are known as SPF.

The goal of this experiment is to determine whether or not the systematic error in the geodetic position determined from TOA and attributable to propagation can be corrected by the application of a correction factor that, in turn, is some function of ECD. To accomplish this goal, three things must be carefully measured: the length of the path over which the propagation is observed, the transit time of the phase, and the position of the pulse envelope with respect to the phase at both ends of the path. Briefly stated, if these measurements are made for many paths,

we should be able to solve the following expression for the desired function of ECD:

$$f(\Delta ECD) = (\Delta D \div C) - \Delta TP, \quad (1)$$

where  $\Delta ECD$  is the change in ECD over the path,  
 $\Delta D$  is the path length,  
 $C$  is the vacuum speed of light,  
 $\Delta TP$  is the transit time of the phase, and  
 $f(\Delta ECD)$  is the desired function.

The right-hand side of Eq. (1) is defined for the purposes of this report to be SPF.

#### RAY PATHS

It was originally planned to equip two mobile test vans with suitable timing and electrical measurement equipment so that a Loran-C pulse could be measured at both ends of any arbitrarily selected ray path at ground level. Although not rigorous in an electrical sense, for planning purposes a ray path is assumed to lie in the plane of a great circle passed through the electrical center of a transmitting antenna. As planning progressed, the USAF test van owned by the Loran System Program Office became available for loan to APL in support of the experiment. For the sake of economy, it was decided not to procure a second van and to locate one set of measurement equipment at a fixed site. NAVOBSY was chosen as the fixed site to facilitate the transfer of time from the Master Clock Ensemble that resides at the Observatory for the purpose of maintaining Universal Time Coordinated (UTC).

The selection of the fixed site restricts the ray paths of interest to those that pass through NAVOBSY. Four such paths are therefore available: those from the Carolina Beach, Jupiter Inlet, Nantucket, and Dana Stations. Since the overland portions of the ray paths from Carolina Beach and Jupiter Inlet are nearly the same, it was decided not to examine the Jupiter Inlet ray. The three ray paths chosen for the experiment are shown in Fig. 1.

#### TEST SITES

Since the NAVOBSY data gathering site is fixed, the field sites that define the other end of each of the propagation paths to be observed must bear an

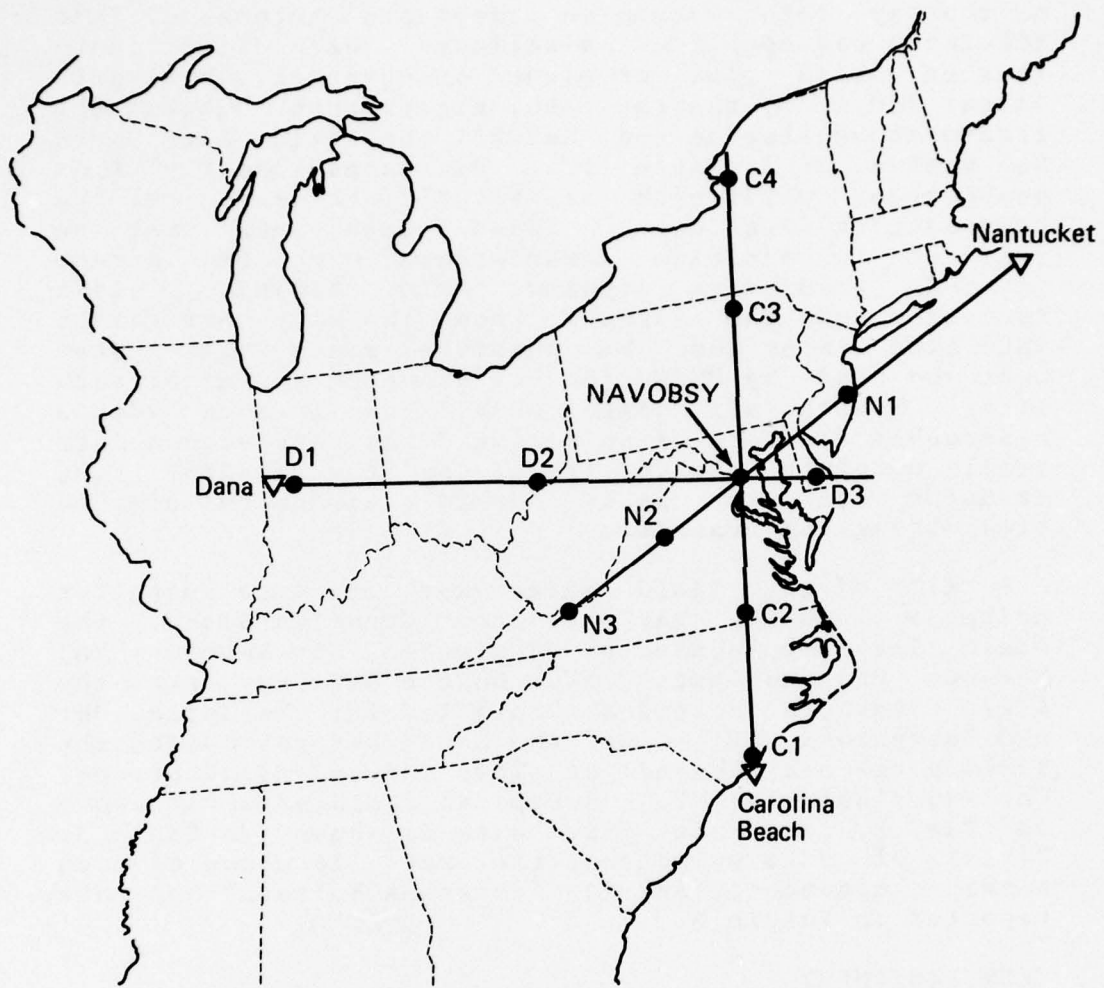


Fig. 1 Locations of Ray Paths and Test Sites

appropriate geometric relationship to NAVOBSY. The first consideration was the lengths of the paths. They should be long enough to expect a significant propagation effect, but not so long as to cause excessive attenuation at the farthest site from the transmitting station. Second, the field sites must be on the ray path within an acceptable tolerance. This tolerance was specified as follows: each field site must be within plus or minus one-quarter wavelength (about 750 m) of the ray path, except that between the transmitting station and NAVOBSY the field sites must be within a distance that decreases linearly from one-quarter wavelength at NAVOBSY to zero at the transmitting station. Third, each site must be selected to minimize interference with the direct Loran-C groundwave signals. In addition, clear reception of the signals from the Navy Navigation Satellite System must be possible since this system must be used by DMATC for the accurate survey of each site. Fourth, all sites should be located within reasonable distance of an airfield that can accommodate small aircraft, since travel by the NAVOBSY time transfer team must be by air to minimize the elapsed time during the transfer.

All of the field sites met the site selection criteria. On the ray path from Carolina Beach, the field sites are located at Wilmington, NC; Emporia, VA; Towanda, PA; and Dexter, NY. On the Dana ray path, the field sites are located at Danville, IN; Marietta, OH; and Georgetown, DE. On the Nantucket ray path, the field sites are located at Toms River, NJ; Grottoes, VA; and Bluefield, WV. A typical field site is shown in Fig. 2, and the fixed site is shown in Fig. 3. Details of site selection, the exact location of each surveyed monument, and the distances between them are reported in Volume B.

#### TEST EQUIPMENT

Equation (1) symbolically represents the goal of the experiment. This equation relates four physical quantities: the length of the propagation path, the vacuum speed of light, the propagation time of the phase, and the change in ECD over the path.

The value of the vacuum speed of light reported in Ref. 10 was adopted for the experiment. It is 299 792 456.2 m/s. The reference also reported a standard deviation of 1.1 m/s. However, a private

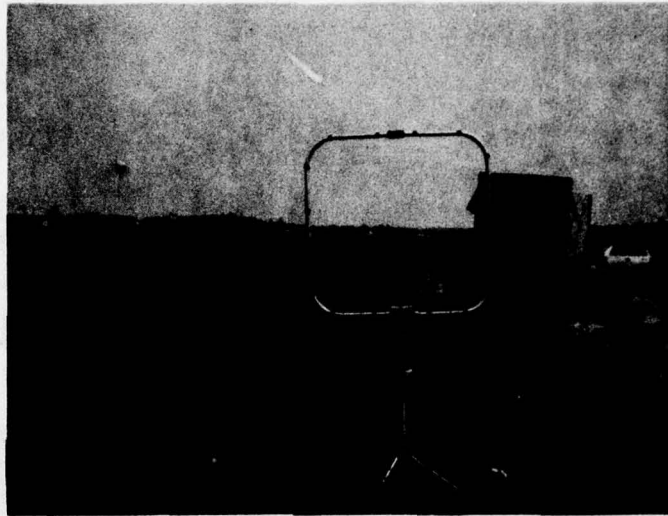


**Fig. 2 View of Field Site at Georgetown, DE**

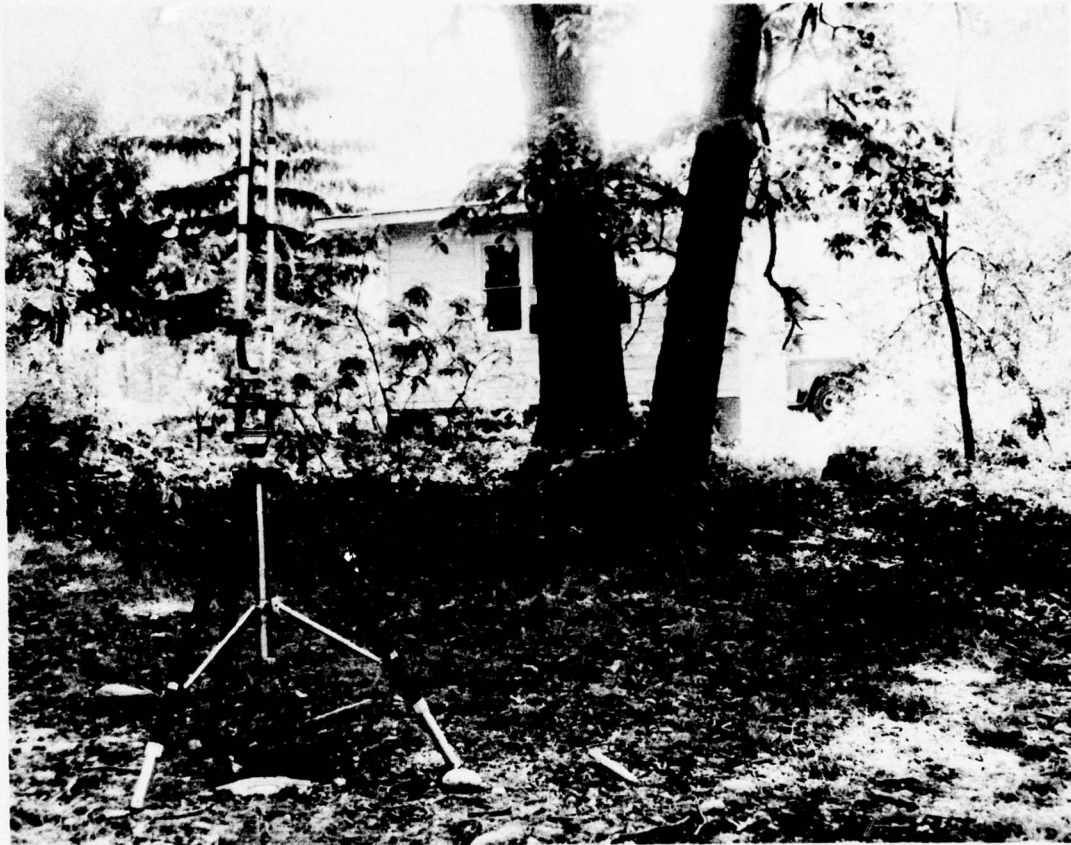


Fig. 3 Loran-C Antenna at NAVOBSY

communication with G. Luther of the National Bureau of Standards indicated that a more recent estimate of the standard deviation is 3.0 m/s attributable to deviations in the length of the meter based on krypton that were not accounted for in the work reported in Ref. 10. Discovery of these overlooked deviations mattered very little since, for the purposes of this experiment, both standard deviations are negligible.

Each of the 10 field sites and the fixed site required precision surveys so that the distance between antennas at either end of the propagation path could be determined. The choice of equipment for accomplishing long distance surveys was easily resolved. Surveys by satellite methods are more timely, less costly, and more accurate than surveys by any other method. Therefore, arrangements were made to engage the satellite surveying services offered by the Defense Mapping Agency. Satellite Observation Teams from the Agency's Topographic Center performed all the surveys using geocivers in the manner reported in Ref. 11. The Topographic Center reports that the standard deviation of each geodetic coordinate, i.e., in the direction of latitude, longitude, and height, is 1 m. Because the measurement errors associated with each position fix are independent of the choice of coordinate system, the standard deviation of error in the computed geodetic distance is 1.4 m (see Volume B).

Propagation time of the phase was expected to be the difference between the TOA of a specific zero crossing in the Loran-C pulse at the beginning of the path and the TOA of the same zero crossing at the end of the path. Obviously, time must be kept with respect to the same reference at both ends. Since the error in distance converts to about 4 ns at the speed of light, keeping of time to comparable accuracy presented a challenge. It was decided, therefore, to refer all time measurements to the Master Clock Ensemble at NAVOBSY. It is this clock system that provides the national standard for UTC. After an investigation of the performance and availability of portable frequency standards, it was decided that low noise cesium frequency standards would be used at the field and fixed sites to keep time and to provide highly accurate time intervals; also a portable clock driven by a low noise cesium frequency standard would be used to transfer UTC from the Master Clock Ensemble to the field and fixed site clocks. An error analysis made

before the experiment was begun indicated that the propagation time over the path could be expected to be determined to an accuracy of 7 ns rms and the change in ECD to 15 ns rms if time transfers to both the field and fixed sites could be accomplished within 12 hours of the time of the loran observations. It was quite fortunate that these errors compared as well as they did to those associated with distance because reasonably portable timing equipment having better stability characteristics was not available.

To accomplish time transfers within the shortest possible time, the portable clock was flown to most of the field sites. NAVOBSY contracted with SAID, Inc., operating out of Dulles International to provide this service. The portable clock was flown to all field sites except Georgetown, DE, which was within acceptable range by automobile. Figure 4 shows one of the SAID aircraft.

Figure 5 is a block diagram of the measurement system that was used. Two identical sets of equipment were assembled, finely tuned, and matched (see Volume C). The equipment used during the experiment is identified in Table 1.

All of the components listed in Table 1 were purchased except the cesium clock and the interface unit. The cesium clocks were furnished by NAVOBSY. The interface unit was designed and constructed at APL.

The interface unit performs a number of functions. It provides means for the operator to enter pertinent data, i.e., characteristics of the environment during the recording, UTC time, and the group repetition interval (GRI). It also provides means for operator control over the recording. Four controls are provided: (1) the recording on-off switch, (2) end-of-file marker, (3) slew switch, and (4) time set switch. The slew switch permits adjustment of the time at which electrical measurements are made so that the measurements occur at desired locations on the Loran-C pulse. The time set switch permits setting the 0.1- $\mu$ s clock to UTC. Internally, the interface unit provides the UTC clock, the GRI counter, and the measurement sample gates. System details, including the documentation of the interface unit, are contained in Volume C.



Fig. 4 Piper Cherokee Aircraft

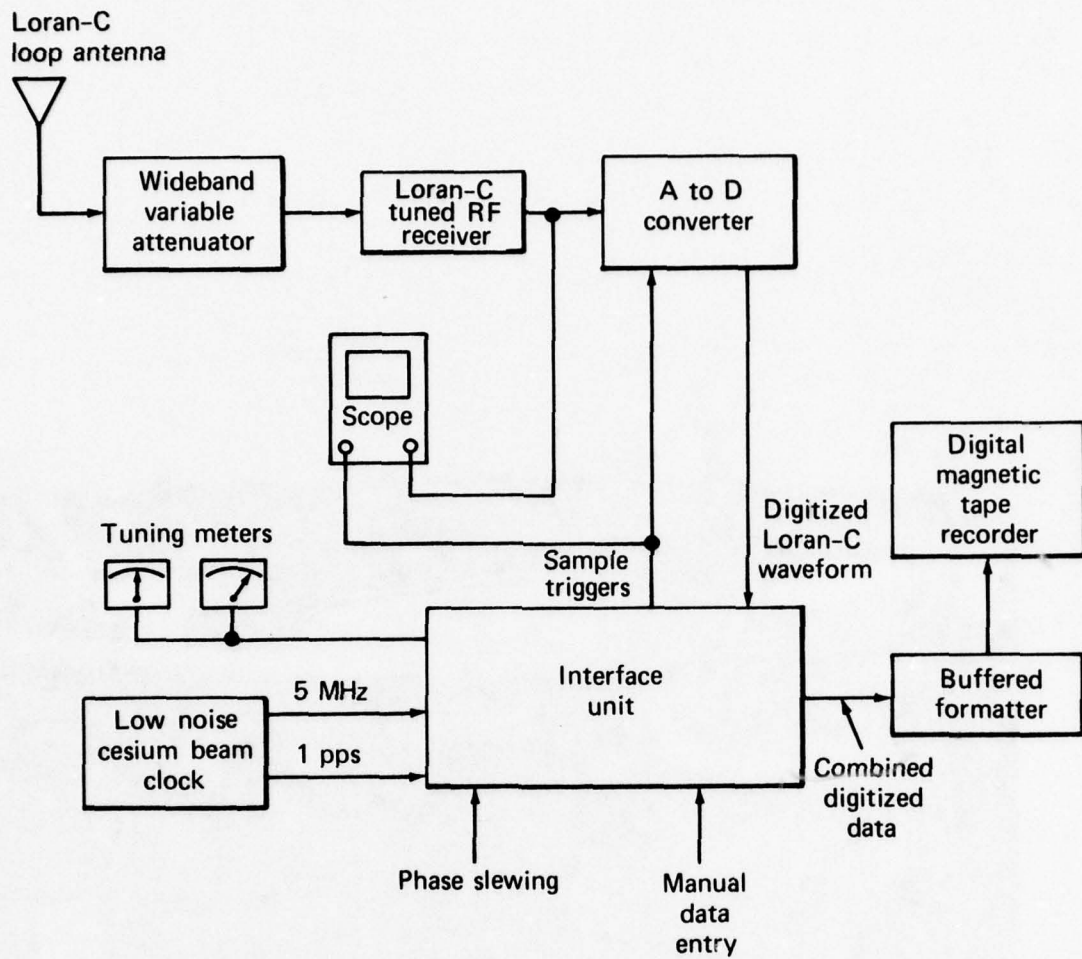


Fig. 5 Functional Block Diagram of the Measurement System

The measurement system installed in a 6-ft rack for use at the fixed site is shown in Fig. 6. The measurement system installed in the van is shown in Fig. 7.

The van (Fig. 8) was a 19 000-lb gross weight truck that had been equipped to support loran field tests. It was loaned to APL by the USAF for this purpose.

Table 1

Equipment Used During the Experiment

Item	Quantity	Model
Loop Antenna	2	Austron 2021L
Receiver	2	Austron 2082
Attenuator	2	Kay Elemetrics 461B
A to D Converter	2	Preston GMAD-1-14B
Tape Recorder	2	Kennedy 9000
Buffered Formatter	2	Kennedy 9232
Counter	1	Hewlett-Packard 5345A
Oscilloscope	1	Tektronix 7603
Oscilloscope	1	Tektronix 545
Cesium Clock	3	Hewlett-Packard E44-5061A
Tuning Meter	4	Triplett 320-G
Interface Unit	2	APL/JHU

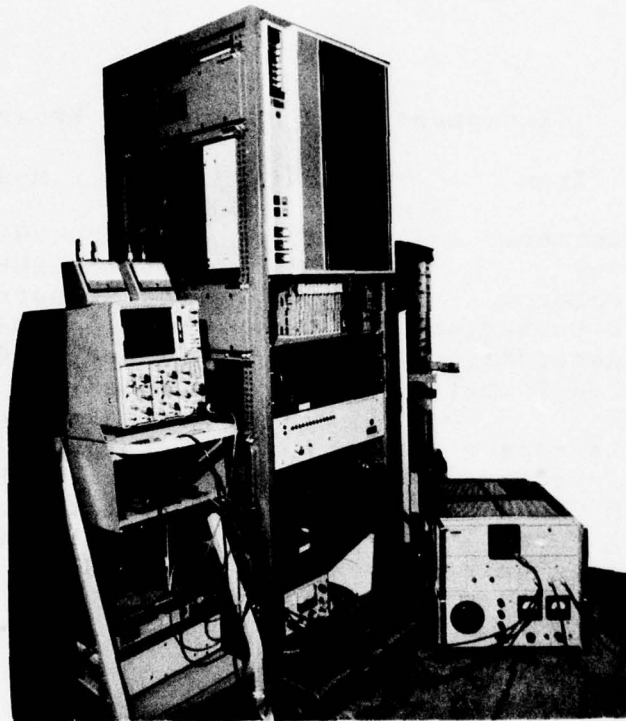


**Fig. 6 Fixed Site Measurement System in NAVOBSY Building No. 54**

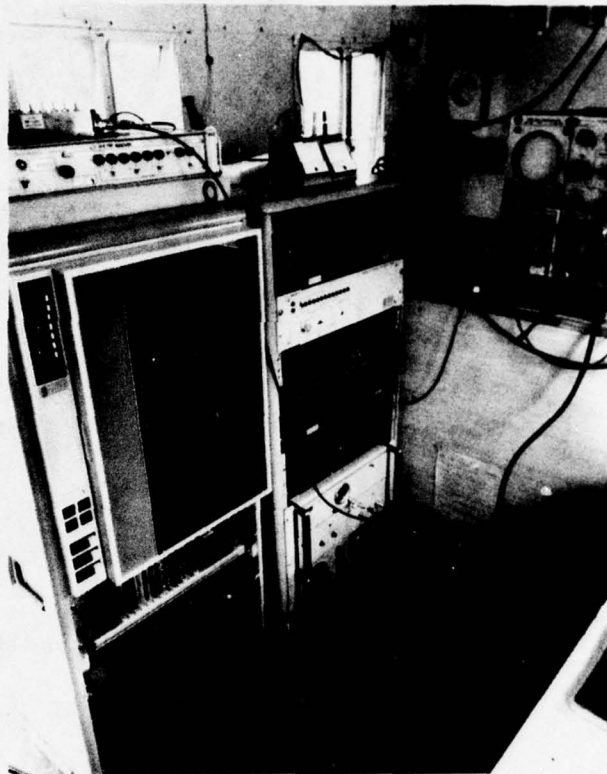


Fig. 7 Field Site Measurement System in USAF Van



Fig. 8 NAVOBSY Building No. 54 and USAF Van

#### 4. TEST OPERATIONS

It was anticipated that the long distances and precision timing that were involved in the experiment would require a high degree of coordination among participants during test operations. Adequate coordination seemed to be achievable if each participant would execute his part of the experiment in accordance with a carefully considered, detailed plan. Such a plan was developed and tested during dry runs at NAVOBSY. The test operations conducted according to the plan are described in Volume B. A summary of these operations follows.

##### SITE SELECTION

Guided by the criteria chosen for the selection of test sites, DMATC selected a number of candidate locations for each site based on information available on existing maps. Each site was then visited by a site selection team of persons from APL, USAF, and DMATC. This team, while on location, selected from among the candidate locations those locations that satisfied the electrical environment criteria described in Section 3. The team also negotiated mutually satisfactory arrangements with the property owners for the placement of a survey monument and for the subsequent occupation of the site for data-gathering purposes. The location thus selected for gathering loran data was marked by installation of a permanent concrete monument topped by a DMA bronze disk. The monument at NAVOBSY is shown in Fig. 9.

##### SITE SURVEYS

Later, each site was occupied for about 1 week by a DMATC Satellite Survey Team. This team recorded the satellite data required to establish the position of the survey monument. All the surveys were completed during the period July through September 1974.

##### LORAN-C MEASUREMENTS

The participants in the experiment during the taking of loran data and the transfer of time were the Project Engineer, T. A. McCarty; the Fixed Site Chief, S. F. Oden; the Field Chief, C. M. DeLoriae; the Analysis Chief, R. R. Smith; and the Time Transfer Chief, W. J. Klepczynski. Each of the participants



Fig. 9 NAVOBSY Survey Monument

developed a check list to be executed before and after data taking to ensure the proper sequence of events.

A typical scenario of events surrounding the taking of test data at each site follows. The day on which data were to be taken was scheduled 1 to 2 weeks in advance. This day was called T-day. The hour during which data were to be recorded (referred to as T-hour) always started at 3:30 PM EDT. The test van arrived at the test site the day before T-day. The Field Chief immediately made arrangements with the property owners for occupation of the site, found the survey monument, set up the loran antenna, checked out the measurement system, and reported its operational availability to the Project Engineer. On T-day, the Field Chief turned on the measurement system well in advance of T-hour, made measurements of the environmental parameters, such as barometric pressure and air temperature, set the UTC clock, and recorded calibration data. These data consisted of measurements of the 100-kHz signal voltage at the output of the cesium frequency standard and then the same signal routed via the loran antenna. These recordings permitted an assessment of the performance of the measurement system immediately prior to the taking of primary data.

Meanwhile, at NAVOBSY on T-day, the Fixed Site Chief turned on his measurement system and executed the same startup procedure as the Field Chief. During the same period, the Time Transfer Chief calibrated his portable clock against the Master Clock Ensemble, moved his clock to the fixed site, calibrated the fixed site clock against the portable clock, and proceeded with his clock to Dulles International for the trip to the field site.

At T-hour, both the Field Chief and Fixed Site Chief started recording loran data and the time, as kept on the UTC clock built into the measurement system. Data were recorded in three 20-min segments starting at T-hour, T-hour plus 21 min, and T-hour plus 42 min. The maximum difference between field and fixed site startup times was 3 s.

The data recorded during the three 20-min periods were referred to as "primary data." They are the data recorded specifically for the development of a correction function for SPF. Ancillary data were also recorded. At each site, recordings were made of the

signals from each transmitter that could be heard. In addition, when the van was located at sites on the Dana ray path, continuous recordings of the Dana signal were made during sunrise and sunset simultaneously at the field and fixed sites. The recordings extended from the beginning of sunrise (or sunset) at the most easterly of the two sites to the end of sunrise (or sunset) at the most westerly.

The Time Transfer Chief arrived at an airport near the field site not long after the end of primary data recording. The Field Chief provided local transportation for the time transfer team and the portable clock. Upon arrival at the field site, the Time Transfer Chief calibrated the van clock against the portable clock, took custody of the primary data field tape, and immediately departed for the return trip to the fixed site. Upon arrival, the fixed site clock was calibrated against the portable clock. He then moved the portable clock to the NAVOBSY Time Service building, where it was calibrated against the Master Clock Ensemble. The longest time required for closure of the time transfer was 13 h. Custody of the primary data tape was transferred to the Fixed Site Chief.

After the equipment was secured at the fixed site, the Fixed Site Chief returned to APL and transferred custody of both the field and fixed site tapes to the Analysis Chief, who subjected the recorded data to the first stage of data reduction. This was accomplished overnight for the purpose of assessing the quality of the data as early on T-day-plus-one as possible. On the basis of this assessment, the Project Engineer instructed the Field Chief to repeat the test or to secure and move to the next site. It was not necessary to repeat the test at any of the sites. The days on which primary data were recorded are given in Table 2.

The label "Baseline" for test field sites means that primary and calibration data were recorded while the van's field site antenna was collocated with the fixed site antenna at NAVOBSY. These recordings permitted the determination of signal transit time through the test equipment, since the loran signal arrived at both antennas at the same time. They also permitted assessment of the ability of both systems to record the same voltage measurements.

Table 2

Test Field Sites Visited

Site	Location	Test Date ( 1975)
Nantucket 1	Toms River, NJ	29 May
Baseline	NAVOBSY, DC	3 June
Dana 3	Georgetown, DE	5 June
Dana 2	Marietta, OH	10 June
Dana 1	Danville, IN	12 June
Nantucket 3	Bluefield, WV	17 June
Nantucket 2	Grottoes, VA	19 June
Carolina 2	Emporia, VA	24 June
Carolina 1	Wilmington, NC	26 June
Carolina 4	Dexter, NY	30 June
Carolina 3	Towanda, PA	2 July
Baseline	NAVOBSY, DC	7 July

## 5. DATA ANALYSIS

### RECORDED DATA

Voltage sampling was done at locations on the loran pulses as shown in Fig. 10. Only the first pulse of each group was sampled, and 32 voltage measurements were taken on each of these pulses. The first 16 were at 2.5- $\mu$ s intervals, and the second 16 were at 7.5- $\mu$ s intervals. In areas of sufficient signal strength, the output of the tuned receiver was adjusted by the wideband attenuator (Fig. 5) to give a pulse amplitude of 0.5 V at the positive peak of the fifth cycle. Otherwise, the attenuator was set no less than 3 dB. The analog-to-digital (A to D) converter then digitized each voltage sample to 13 bits plus a sign bit. The digitized waveforms, along with the time of the first sample point from the UTC clock and manual input information stored in digiswitches, were formatted by a digital formatter and stored on computer-compatible magnetic tape. The tape block size, i.e., the number of eight-bit characters writable in one continuous block, was 512. This number of characters allowed sample point values from seven Loran-C pulses, a UTC clock time, and the information stored in the digiswitches to be stored in each block. The parameters recorded are listed in Table 3 along with their units and numerical range. The standardized format is shown in Fig. 11.

During the recording of calibration data, the odd-numbered sample points were positioned as close as possible to the zero crossings of the 100-kHz output of the cesium frequency standard; for the 100-kHz calibration via the antenna, the sample points were slewed so that samples would be taken only when loran pulses were not present. By inspection of these data, it was easily determined whether or not both sets of test equipment had retained their calibrations since the last baseline test. Throughout test operations, there was no indication of any changes in calibration of either set of test equipment (see Volume B for details of the calibration procedure).

Received loran signals are contaminated by noise. In this report, "noise" is defined to include unwanted signals of any origin, e.g., atmospheric noise, galactic noise, receiver noise, transmitter jitter, and man-made signals. The effect of noise on the raw data

Carolina Beach signal  
observed at Wilmington, NC.

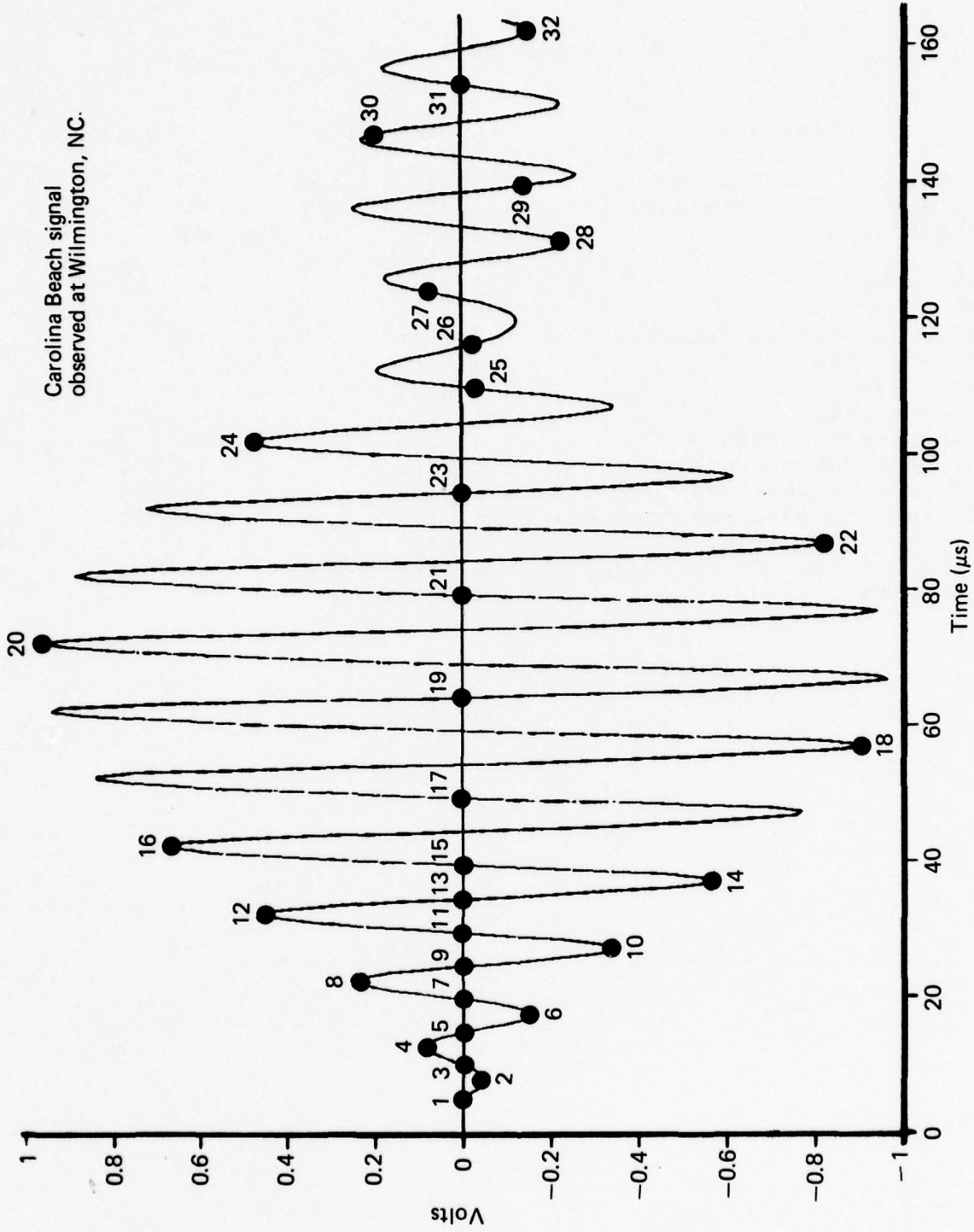


Fig. 10 Typical Loran-C Pulse Showing the Location of Voltage Samples

Table 3

Taped Data

Parameter	Digits/Bits	Units
Voltage at Odd Samples, x	13 bits + sign	V
Voltage at Even Samples, y	13 bits + sign	V
Attenuation	2 digits	dB
Time	13 digits	h, min, $10^{-7}$ s
Day Number	3 digits	-
Year	1 digit	-
Group Repetition Interval	3 digits	$10^{-4}$ s
Station Code	1 digit	-
Site Code	2 digits	-
Weather Code	2 digits	-
Atmospheric Pressure	5 digits	$10^{-3}$ in. Hg
Wet Bulb Temperature	3 digits	$10^{-1}$ °C
Dry Bulb Temperature (outside)	3 digits	$10^{-1}$ °C
Dry Bulb Temperature (inside)	3 digits	$10^{-1}$ °C
Data Recording Mode	1 digit	-
Predicted Time Calibration	9 digits + sign	$10^{-9}$ s
Note Code	1 digit	-

Byte	MSB	LSB	(most/least significant bit)
1	±	x	} (112 pairs of x, y samples, 7 GRI's, in 2's complement binary)
2	x	x	
3	±	y	
4	y	y	
448	±	y	} UTC time of first x sample in block)
449	y	y	
	Hour (10 <sup>1</sup> )	Hour (10 <sup>0</sup> )	
	Minute (10 <sup>1</sup> )	Minute (10 <sup>0</sup> )	
	Second (10 <sup>1</sup> )	Second (10 <sup>0</sup> )	
	Second (10 <sup>-1</sup> )	Second (10 <sup>-2</sup> )	
	Second (10 <sup>-3</sup> )	Second (10 <sup>-4</sup> )	
	Second (10 <sup>-5</sup> )	Second (10 <sup>-6</sup> )	
455	Second (10 <sup>-7</sup> )	---	
	Atten. (10 <sup>0</sup> )	Atten. (10 <sup>1</sup> )	
	PTC (10 <sup>-1</sup> )	PTC (±)	} (PTC = predicted time calibration)
	PTC (10 <sup>-3</sup> )	PTC (10 <sup>-2</sup> )	
	PTC (10 <sup>-5</sup> )	PTC (10 <sup>-4</sup> )	
460	PTC (10 <sup>-7</sup> )	PTC (10 <sup>-6</sup> )	
	PTC (10 <sup>-9</sup> )	PTC (10 <sup>-8</sup> )	
	Day (10 <sup>1</sup> )	Day (10 <sup>2</sup> )	
	Year	Day (10 <sup>0</sup> )	
	Mode	Xmitter	
	Site (10 <sup>0</sup> )	Site (10 <sup>1</sup> )	
	Wx (10 <sup>0</sup> )	Wx (10 <sup>1</sup> )	
	DBTI (10 <sup>1</sup> )	Note	} (DBTI = inside dry bulb temperature) (WBT = wet bulb temperature) (DBT = outside dry bulb temperature)
	DBTI (10 <sup>-1</sup> )	DBTI (10 <sup>0</sup> )	
470	WBT (10 <sup>0</sup> )	WBT (10 <sup>1</sup> )	
	WBT (10 <sup>-1</sup> )	WBT (10 <sup>-1</sup> )	
	DBT (10 <sup>1</sup> )	DBT (10 <sup>0</sup> )	} (BARO = barometric pressure)
	DBT (10 <sup>-1</sup> )	DBT (10 <sup>0</sup> )	
	BARO (10 <sup>0</sup> )	BARO (10 <sup>1</sup> )	
	BARO (10 <sup>-2</sup> )	BARO (10 <sup>-1</sup> )	
475	---	BARO (10 <sup>-3</sup> )	} (--- = zero-filled characters)
	GRI (10 <sup>-2</sup> )	GRI (10 <sup>-1</sup> )	
	GRI (10 <sup>-4</sup> )	GRI (10 <sup>-3</sup> )	
512	---	---	

Fig. 11 Raw Data Tape Format for Each Block of Recording

recorded on the magnetic tape is not linear with amplitude. The A to D converters were adjusted so that a signal of 1 V produced the largest binary output number, i.e., 2 to the 13th power minus one. Therefore, the actual noise level associated with 1-V recordings cannot be determined from the data. As an additional consideration, the possibility existed that the recording might contain some very large false recordings due to an intermittent recording malfunction. Therefore, judgment of the quality of recorded data was made after each recording by inspection of data that survived a first-stage editing process. In this process, all the data recorded for a single pulse were discarded if the absolute value of any of the samples of voltage for that pulse equalled or exceeded 1 V, and a record was kept of the number of pulses discarded.

Editing at this level is complementary to the final goal of obtaining the best possible estimate of the uncontaminated loran signal. However, having edited the data, it is then impossible to determine the signal-to-noise (S/N) ratio at the antenna. Nevertheless, the S/N ratios of the edited data are quite interesting.

Table 4 lists the S/N ratio computed from data taken simultaneously at each field test site and NAVOBSY and subjected to first- and second-stage editing. Stage 1 editing level, as mentioned, is at plus or minus 1 V. Stage 2 editing is like stage 1 except that the level is at plus or minus two times the standard deviations of the data that survived stage 1 editing.

The signal voltage used in the S/N ratios in Table 4 is the mean value of sample point 12 (i.e., 32.5  $\mu$ s into the pulse) during the first 20-min recording (i.e., data segment 1). The noise voltage used is the standard deviation of the voltage about the mean at sample point 12. Note that the S/N ratio at Dexter, NY, is 3 dB (stage 1) and 5 dB (stage 2) greater than that at NAVOBSY, even though Dexter is more than twice the distance from Carolina Beach as NAVOBSY. On the other hand, Towanda is beyond NAVOBSY but closer than Dexter, and the S/N ratio is 9 dB (stage 1) and 12 dB (stage 2) less than that at NAVOBSY. Note also that the S/N ratios vary from 3 to 32 dB (stage 1) and 8 to 34 dB (stage 2). The difference between the stage 1 and stage 2 S/N ratios varies from 0 to 7 dB, whereas a

Table 4

Signal-to-Noise Ratio of the Primary Data from  
 Measurements at the 12th Sample Point

1975 Day No.	Site	Transmitting Station	Station to Site (m)	Edited Data Stage 1 S/N(dB)	Stage 2 S/N(dB)
177	Wilmington, NC NAVOBSY	Carolina Beach	23 572	32	34
177		Carolina Beach	544 244	21	24
175	Emporia, VA NAVOBSY	Carolina Beach	293 344	30	33
175		Carolina Beach	544 244	23	26
183	Towanda, PA NAVOBSY	Carolina Beach	867 731	10	11
183		Carolina Beach	544 244	19	23
181	Dexter, NY NAVOBSY	Carolina Beach	1 113 946	21	23
181		Carolina Beach	544 244	18	18
163	Danville, IN NAVOBSY	Dana	85 946	32	34
163		Dana	903 083	7	9
161	Marietta, OH NAVOBSY	Dana	526 905	30	32
161		Dana	903 083	8	9
156	Georgetown, DE NAVOBSY	Dana	1 053 517	3	8
156		Dana	903 083	4	8
149	Toms River, NJ NAVOBSY	Nantucket	384 346	22	27
149		Nantucket	657 576	6	9
170	Grotooes, VA NAVOBSY	Nantucket	827 590	8	15
170		Nantucket	657 576	13	20
168	Bluefield, WV NAVOBSY	Nantucket	1 063 425	7	11
168		Nantucket	657 576	14	16

constant improvement would be expected if the character of the noise were the same everywhere. Table 4 clearly indicates that the predominant influence on S/N ratio is the local electrical environment.

The statistical problems presented by signals contaminated by noise have been treated extensively in published literature. A definitive interpretation of this wealth of knowledge with respect to the data taken is beyond the scope of this summary; however, one principle is clear: in the presence of non-negligible noise, high confidence in the definition of the extracted signal can only be achieved if the noise can be characterized with high confidence.

To achieve some understanding of the noise content of the data, histograms were drawn using data obtained at sample points 11 and 12. These points are in-quadrature (Q) and in-phase (I) samples, respectively, 30 and 32.5  $\mu$ s into the loran pulse. Figure 12 presents a two-dimensional histogram of these I and Q samples at Danville, IN. It also presents two marginal (one-dimensional) histograms, one each for I and Q. These histograms are drawn for all the first-stage edited data inside  $\pm 6$  standard deviations from the average of the data in each direction. Included also at the bottom of each histogram is a table of parameters and their values that apply to the histogram. The "Total Number of Pairs" is the total number of paired values of I and Q that were considered for the histogram. The "T11,12 Edit Sigma" is the average of the standard deviations of the first-stage edited data for I and Q. The "Edit Level" is the number of average standard deviations about the mean within which the points inside the histogram fall. The sum of "T11 Edit Pairs," "T12 Edit Pairs," and "T11,12 Edit Pairs" is the number of points that fall outside the histogram. The "T11 Average" and "T12 Average" are the average values of Q and I, respectively, inside the histogram in tens of volts. Figure 13 displays the same information from data taken simultaneously at NAVOBSY.

In the absence of noise, all the sample points of the histograms would fall in the center bin. Obviously, this is not the case. Careful inspection of Fig. 12 indicates that the dense cluster of data points surrounding the center fits a normal distribution reasonably well. This is best shown by testing the I and Q marginal histograms of Fig. 12 against a normal distribution.





Figure 13, however, is more complicated. The cluster of sample points about the center exhibits elliptical contours that are inclined at about  $135^\circ$ . Furthermore, it is bimodal (double-humped) along the  $135^\circ$  axis, and the outlying points are more numerous than would be expected from a two-dimensional normal. This seems to indicate that the noise includes contamination from at least three different sources having different probability distributions. The impact of this will be discussed later in more depth.

Having examined all of the histograms of first-stage edited data, it was decided that significant additional improvement could be obtained with additional editing. The centrally located cluster of points did not extend appreciably beyond two standard deviations in any case. It was this observation that led to the second-stage editing level of two standard deviations referred to earlier. Of the 12 000 pulses sampled during a 20-min period, editing threw out 1180 to 5500 pulses, depending on the character of the noise. All subsequent data analysis was done using data that had been subjected to second-stage editing.

#### OBSERVED SIGNAL

At this point, it appeared that the best estimate of the true signal voltage at each of the 32 sample points on the pulse was the mean of the stage 2 edited data. These mean voltages were computed for each of the three 20-min segments of data taken at each field site and at NAVOBSY. The number of voltage samples averaged for each sample point varied from 6500 to 10 800.

Recall that the signal voltage was sampled at  $2.5\text{-}\mu\text{s}$  intervals for the first 16 samples and then at  $7.5\text{-}\mu\text{s}$  intervals for the next 16. Also, only the first pulse in each group of eight was sampled. The sample points were very accurately timed from the 5-MHz reference signal of the cesium standard. They were positioned on the pulse so that odd-numbered samples occurred as near as possible to zero crossings. These samples were labeled "Q" and the even samples "I." Sample No. 11 was placed near the zero crossing at the end of the third cycle. Since the Q and I samples are orthogonal at 100 kHz, the observed values of Q and I are samples of the modulations of the cosine and sine,

respectively. That is to say,

$$V(t-t_0) = I(t-t_0)\sin(\omega(t-t_0)+\phi) + Q(t-t_0)\cos(\omega(t-t_0)+\phi), \quad (2)$$

where  $V$  is the signal voltage,  
 $I(t-t_0)$  is the sine modulation,  
 $Q(t-t_0)$  is the cosine modulation,  
 $\omega$  is the angular frequency,  
 $\phi$  is the phase angle measured at  $t_0$ ,  
 $t_0$  is the reference time, and  
 $t$  is time.

As this equation relates to the test, the modulation functions  $I(t-t_0)$  and  $Q(t-t_0)$  are determined by the I and Q measurements,  $\omega$  is two times pi times 100 kHz by definition,  $t$  is the variable,  $t_0$  is the time of the first sample point, and  $\phi$  is the arctangent of I divided by Q at  $t$  equals  $t_0$ .

To accommodate analysis of the data by computer, it was necessary to define analytic representations of  $Q(t-t_0)$  and  $I(t-t_0)$ . After extensive experimentation with exponential and polynomial fits, it was found that the leading edge of the pulse could be fitted best if polynomials were used and the coefficients of the zeroth and first power of  $t$  were constrained to be zero. This forces both the value and the slope of the leading edge at zero to be zero and accommodates leading edge shapes that are controlled to a template of the form  $t^2e^{-kt}$ . In addition, it was found that 10th degree polynomials were required to cause the largest residuals to fall inside the standard deviation of the data. Therefore, 10th degree fits were adopted as the standard representation of the sine and cosine modulations for all of the data.

Inspection of the numerical data early in the test had indicated substantial values of Q, but this observation was not disturbing at the time because the sample points could only be set with a resolution of 0.1  $\mu$ s, and, therefore, some Q was always expected. However, when the analytic form of  $Q(t-t_0)$  and  $I(t-t_0)$  had been determined, it was not possible to find any value of  $\phi$  in Eq. (2) that made  $Q(t-t_0)$  negligible at any of the sites. Since  $Q(t-t_0)$  could have been made negligible by a phase shift (especially using data taken close to the transmitters), had the transmitters been transmitting pure amplitude modulation (AM) of the

carrier (as indicated in most reference material, e.g., Refs. 1, 12, and 13), it can be concluded that the signal being transmitted includes modulation other than AM.

Equation (2) was solved, therefore, for a value of  $\phi$  that produced a minimum amount of energy in the cosine modulation in the range of  $t$  from 10 to 70  $\mu\text{s}$ , and the I and Q polynomials were re-referenced to zero by the time increment corresponding to the phase shift. This range of  $t$  was chosen because critical control of the transmitter is exercised only over the leading edge of the pulse, and observations of the pulse earlier than 10  $\mu\text{s}$  are very small in amplitude. Figures 14 and 15 display the results obtained from the data taken at Wilmington, NC, and Dexter, NY, both of which describe pulses from Carolina Beach. Figure 16 shows the results from data taken at Danville, IN, on pulses from Dana, and Fig. 17 from data taken at Toms River, NJ, on pulses from Nantucket. Comparison of the Wilmington and Dexter results shows the effects of propagation. These results, together with the Danville and Toms River results, show similar behavior among all three transmitters. The pulse envelope shapes corresponding to Figs. 14 through 17 are shown in Figs. 18 through 21.

It will be observed in Figs. 14 through 17 that the cosine modulation is small compared to the sine modulation. In terms of volts at  $t$  equal to 30  $\mu\text{s}$ , the ratio of cosine to sine modulations varies from 6 to 16% for the cases shown. It varies from 3 to 25% over all the observations made during the test. Therefore, the largest observed effect of the cosine modulation on envelope voltage at 30  $\mu\text{s}$  was 3%. However, its effect on the position of the zero crossings within the pulse is quite significant. Table 5 lists the time of occurrence of the zero crossings when all the zero crossings at the end of the third cycle are aligned. Note that none of the intervals between the zero crossings are 10  $\mu\text{s}$ , as they would be if the 100-kHz carrier was pure-amplitude modulated. The more significant observation, however, is that the TOA measured by a receiver that is perfectly tracking the standard third-cycle zero crossing reflects the influence of propagation on the cosine modulation that is not accounted for in the classical definitions of SPF.

LORAN-C SIGNAL VOLTAGE PLOTTED AGAINST TIME IN MICROSECONDS  
 FIELD SITE: WILMINGTON, NC STATION: CAROLINA BEACH XMTR: 19 DATA SEGMENT: ONE  
 ATTENUATION: 28.229 DB AT NAVOBSY, 56.094 DB AT FIELD SITE

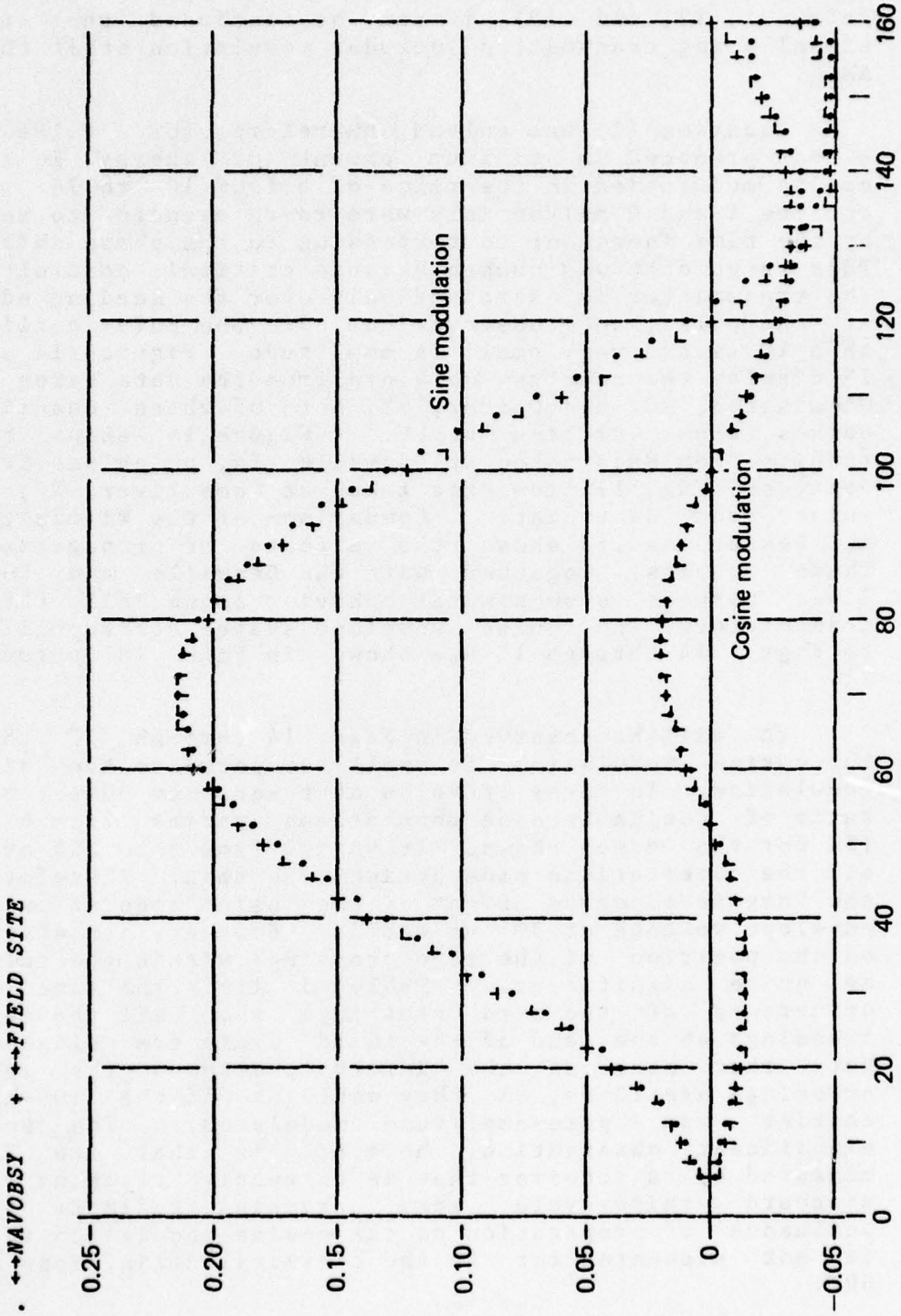


Fig. 14 Sine and Cosine Modulation Observed Simultaneously at  
 Wilmington, NC, and NAVOBSY

LORAN-C SIGNAL VOLTAGE PLOTTED AGAINST TIME IN MICROSECONDS  
1975 DAY NO.: 181  
FIELD SITE: DEXTER, NY STATION: CAROLINA BEACH XMTR: 19 DATA SEGMENT: ONE  
ATTENUATION: 28.393 DB AT NAVOBSY, 8.755 DB AT FIELD SITE

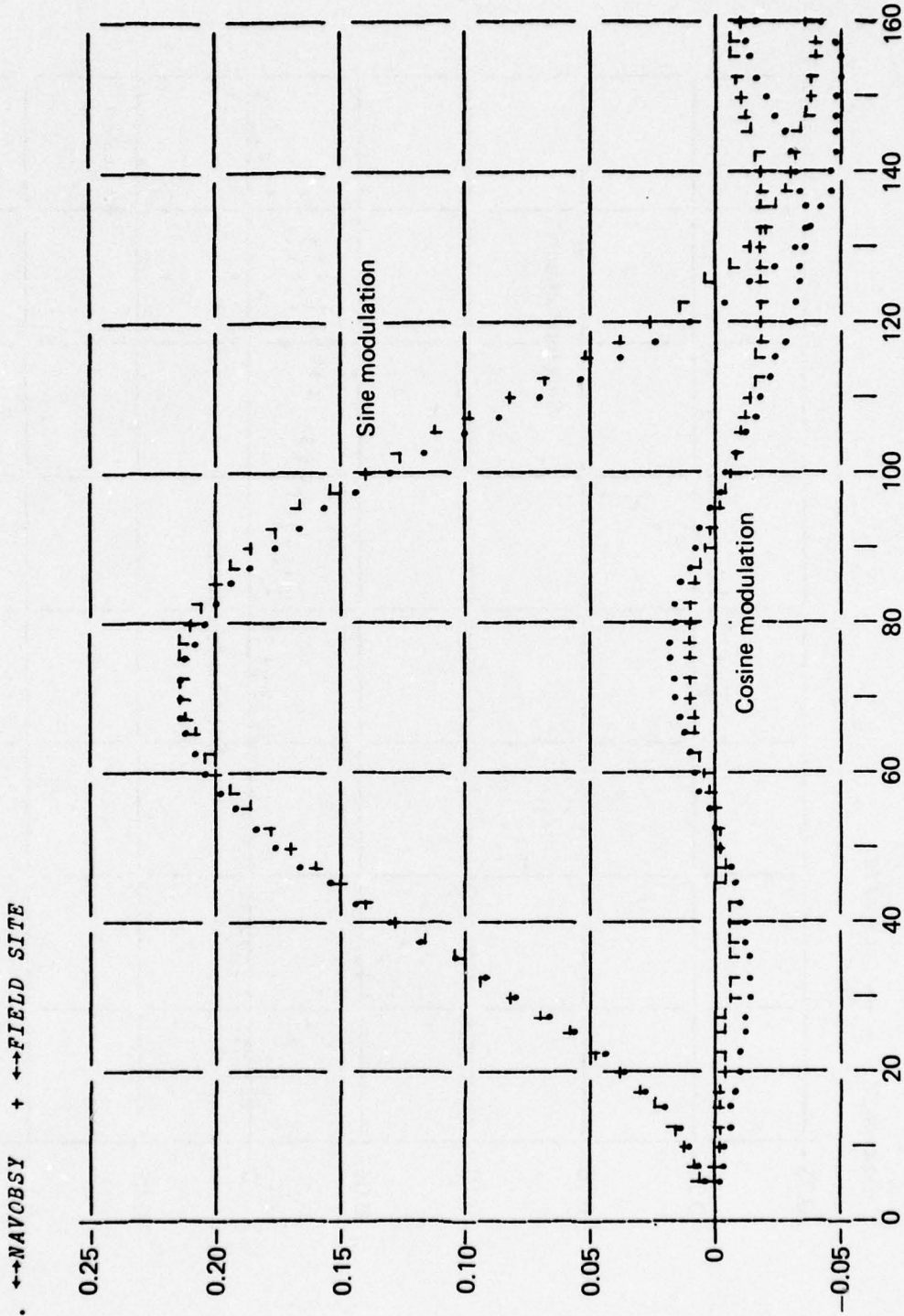


Fig. 15 Sine and Cosine Modulation Observed Simultaneously at Dexter, NY, and NAVOBSY

LORAN-C SIGNAL VOLTAGE PLOTTED AGAINST TIME IN MICROSECONDS  
FIELD SITE: DANVILLE, IN STATION: DANA XMTR: 19 DATA SEGMENT: ONE  
ATTENUATION: 11.072 DB AT NAVOBSY, 41.057 DB AT FIELD SITE

. ↔ NAVOBSY + ↔↔ FIELD SITE

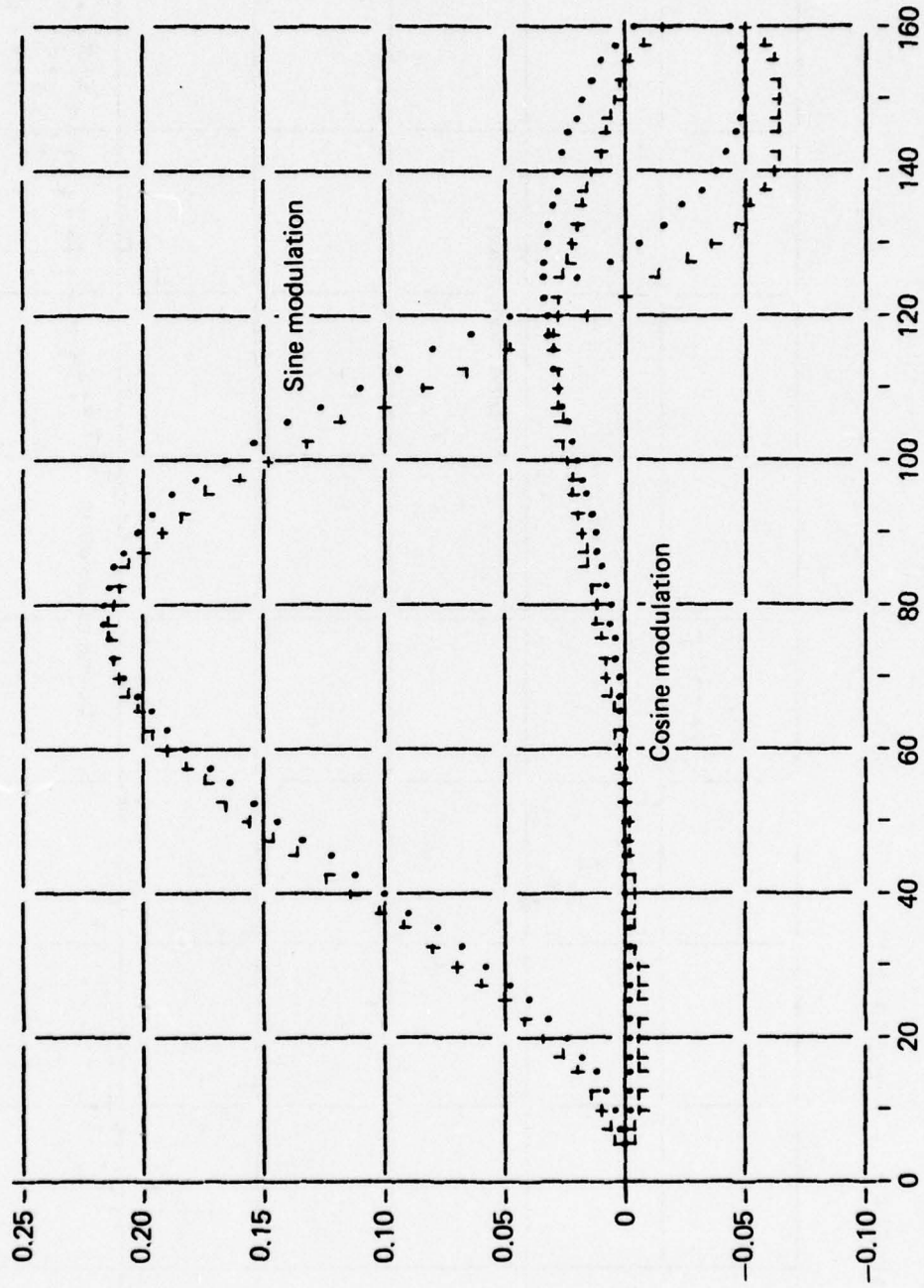


Fig. 16 Sine and Cosine Modulation Observed Simultaneously at Danville, IN, and NAVOBSY

LOBAN-C SIGNAL VOLTAGE PLOTTED AGAINST TIME IN MICROSECONDS  
FIELD SITE: TOMS RIVER, NJ STATION: NANUCKET XMTR: 23 DATA SEGMENT: ONE  
ATTENUATION: 18.975 DB AT NAVOBSY, 24.768 DB AT FIELD SITE

. ↔NAVOBSY + ↔FIELD SITE

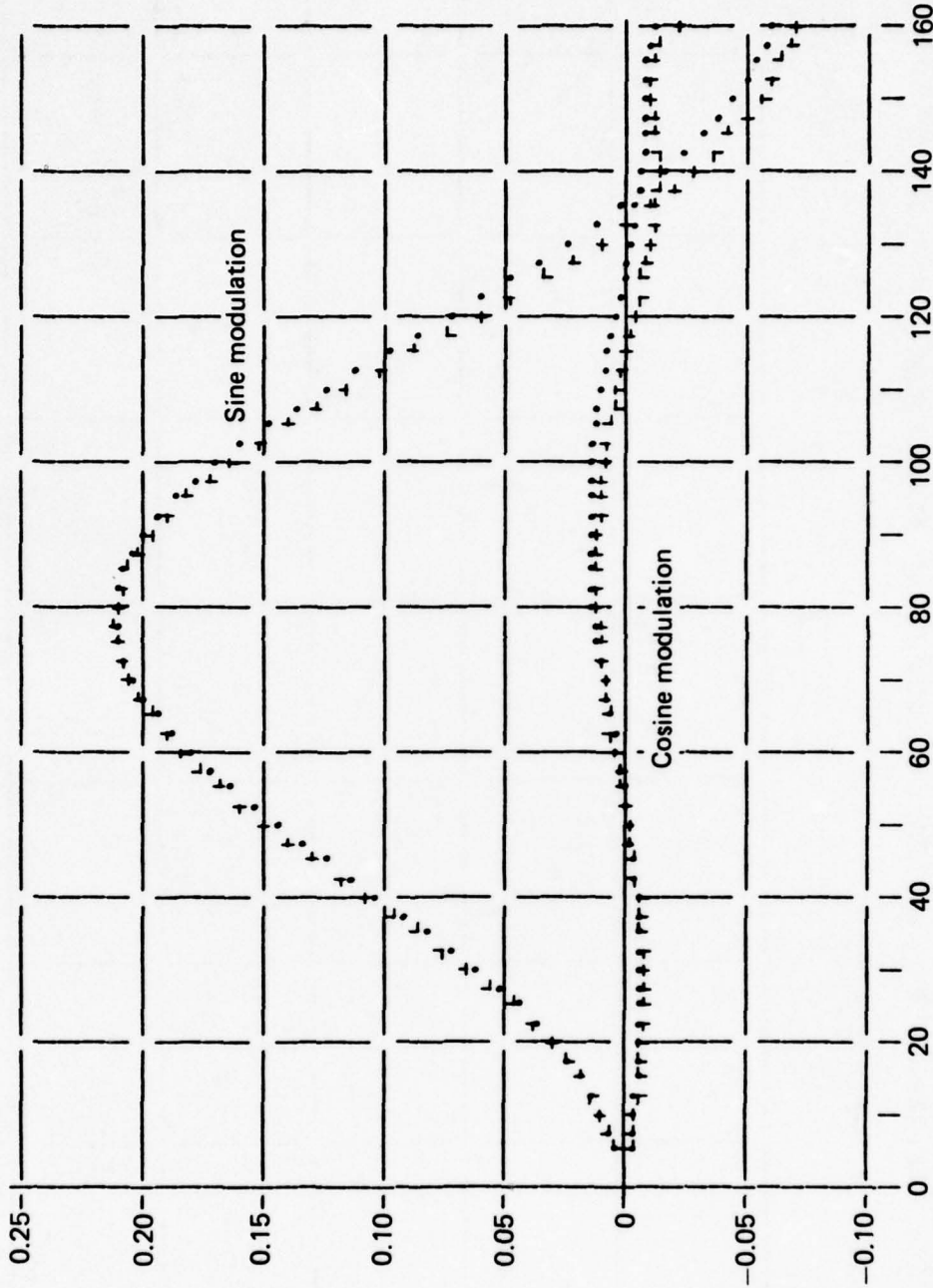


Fig. 17 Sine and Cosine Modulation Observed Simultaneously at  
Toms River, NJ, and NAVOBSY

LORAN-C SIGNAL VOLTAGE PLOTTED AGAINST TIME IN MICROSECONDS  
 FIELD SITE: WILMINGTON, NC STATION: CAROLINA BEACH XMTR: 19 DATA SEGMENT: ONE  
 ATTENUATION: 28.229 DB AT NAVOBSY, 56.094 DB AT FIELD SITE

. ↔NAVOBSY + ↔FIELD SITE

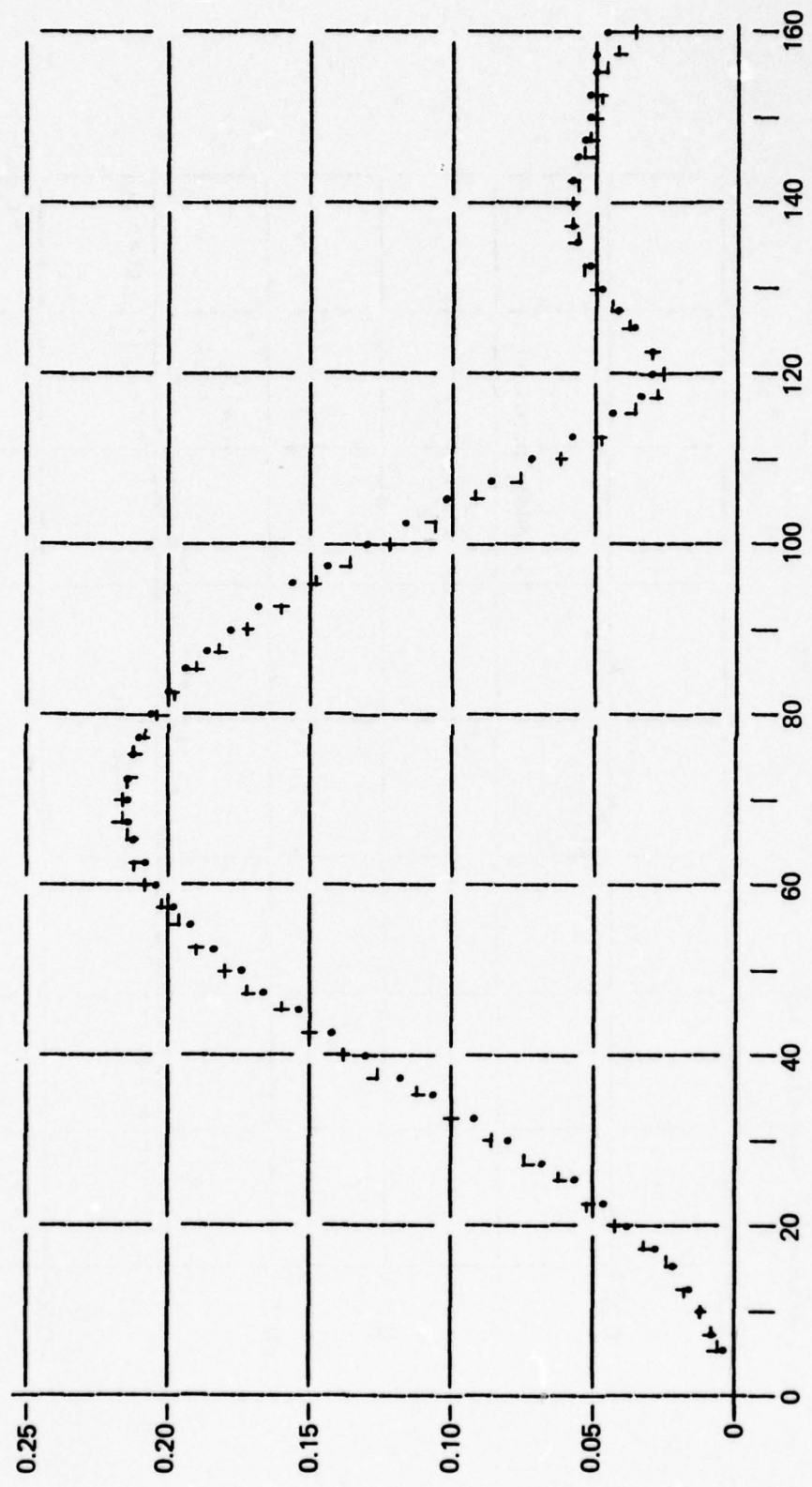


Fig. 18 The Carolina Beach Pulse Envelope at Wilmington, NC, and NAVOBSY

LORAN-C SIGNAL VOLTAGE PLOTTED AGAINST TIME IN MICROSECONDS  
 FIELD SITE: DEXTER, NY STATION: CAROLINA BEACH XMTR: 19 DATA SEGMENT: ONE  
 ATTENUATION: 28.393 DB AT NAVOBSY, 8.755 DB AT FIELD SITE

. ↔ NAVOBSY + ↔ FIELD SITE

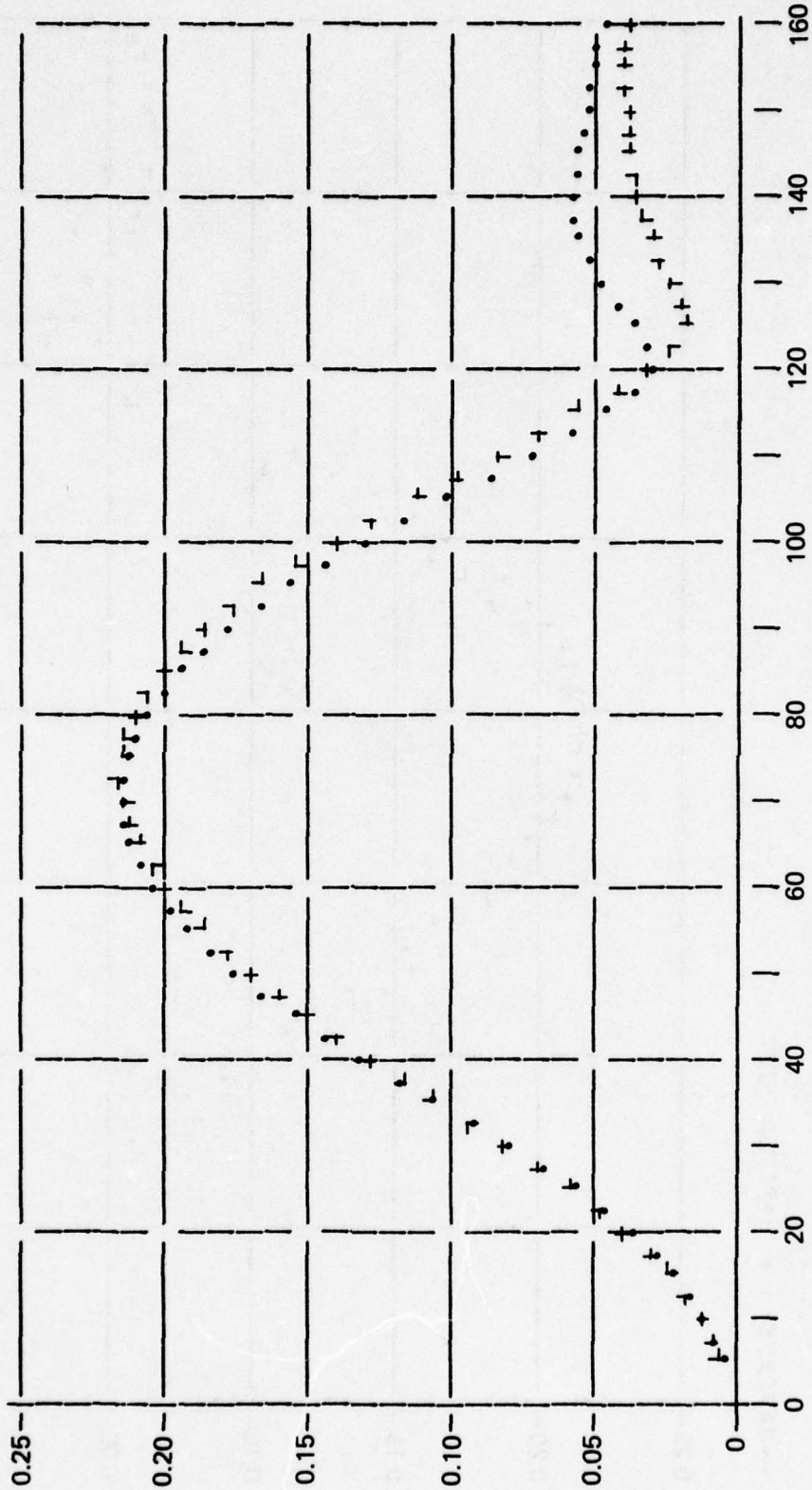


Fig. 19 The Carolina Beach Pulse Envelope at Dexter, NY, and NAVOBSY

LORAN-C SIGNAL VOLTAGE PLOTTED AGAINST TIME IN MICROSECONDS  
 FIELD SITE: DANVILLE, IN STATION: DANA XMTR: 19 DATA SEGMENT: ONE  
 ATTENUATION: 11.072 DB AT NAVOBSY, 41.057 DB AT FIELD SITE

1975 DAY NO.: 163

. ↔NAVOBSY + ↔FIELD SITE

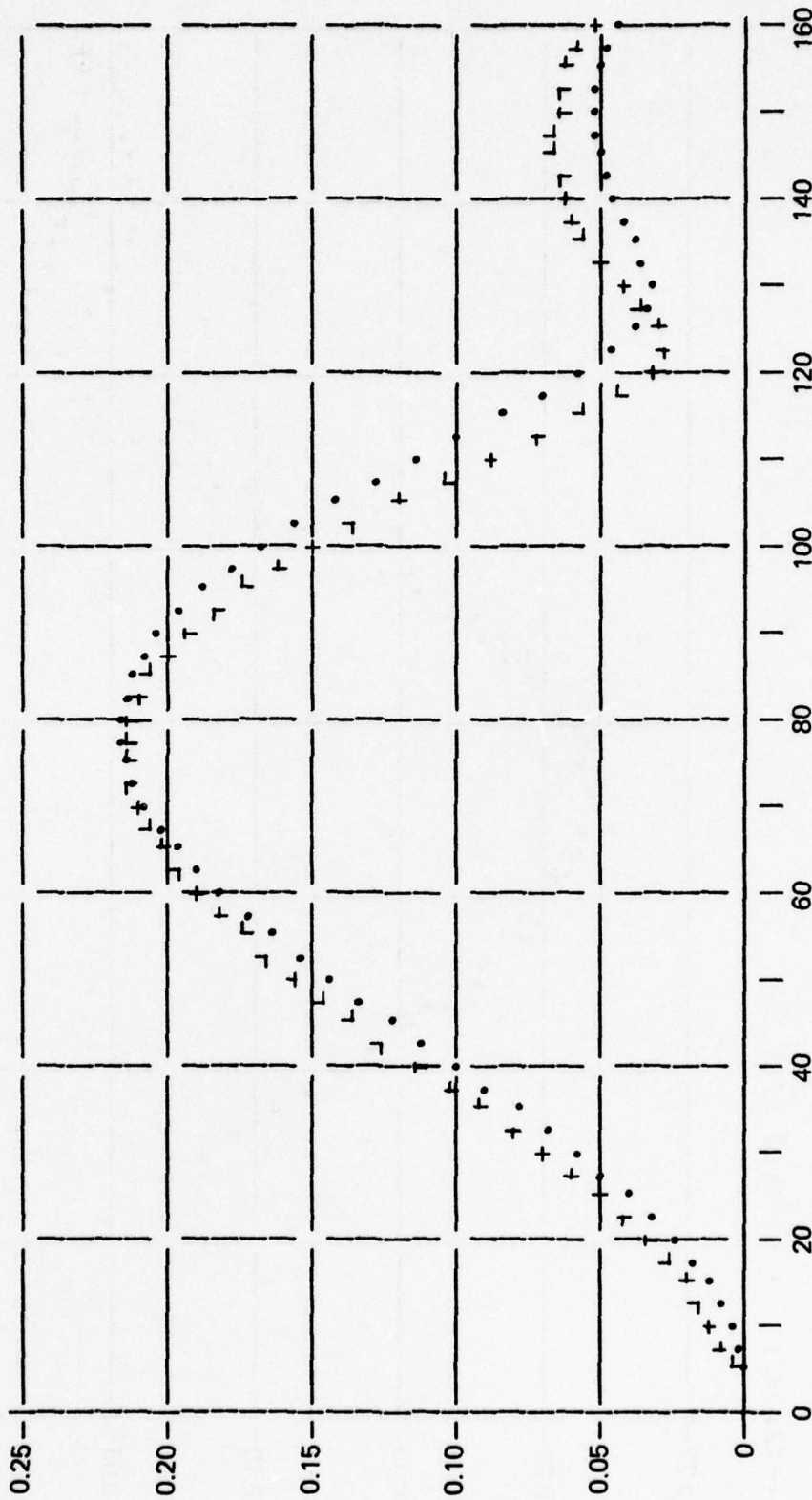


Fig. 20 The Dana Pulse Envelope at Danville, IN, and NAVOBSY

LORAN-C SIGNAL VOLTAGE PLOTTED AGAINST TIME IN MICROSECONDS  
 FIELD SITE: TOMS RIVER, NJ STATION: NANTUCKET XMTR: 23 DATA SEGMENT: ONE  
 ATTENUATION: 18.975 DB AT NAVOBSY, 24.768 DB AT FIELD SITE

. ↔ NAVOBSY + ↔ FIELD SITE

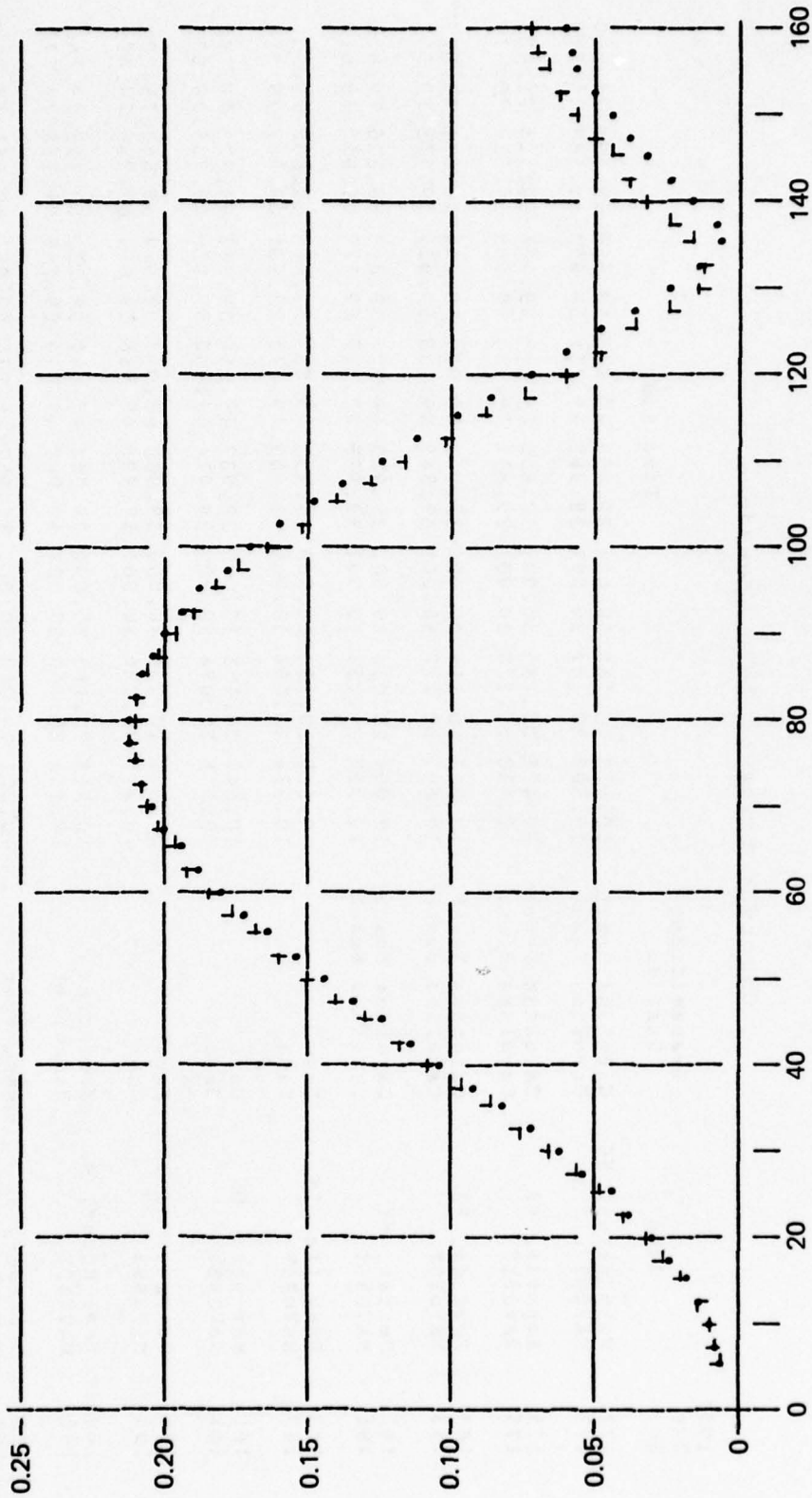


Fig. 21 The Nantucket Pulse Envelope at Toms River, NJ, and NAVOBSY

Table 5  
 Observed Times of Zero Crossings

1975 Day No.	Site	Transmitting Station	Time ( $\mu$ s)
177	Wilmington, NC	Carolina Beach	10.473 20.186 30.001 39.862 49.749 59.658 69.598 79.580
177	NAVOBSY	Carolina Beach	10.403 20.167 30.001 39.868 49.751 59.652 69.587 79.570
175	Emporia, VA	Carolina Beach	10.474 20.185 30.001 39.850 49.718 59.606 69.525 79.483
175	NAVOBSY	Carolina Beach	10.430 20.178 30.001 39.851 49.718 59.603 69.517 79.470
183	Towanda, PA	Carolina Beach	10.341 20.114 30.000 39.918 49.832 59.744 69.671 79.625
183	NAVOBSY	Carolina Beach	10.601 20.227 30.001 39.849 49.729 59.634 69.572 79.549
181	Dexter, NY	Carolina Beach	10.064 20.030 30.001 39.973 49.926 59.868 69.826 79.823
181	NAVOBSY	Carolina Beach	10.357 20.153 30.001 39.875 49.767 59.677 69.622 79.615
163	Danville, IN	Dana	10.615 20.159 30.000 39.938 49.899 59.864 69.830 79.791
163	NAVOBSY	Dana	10.378 20.066 30.001 39.983 49.975 49.965 69.947 79.918
161	Marietta, OH	Dana	10.544 20.155 30.000 39.937 49.898 59.862 69.823 79.774
161	NAVOBSY	Dana	10.735 20.094 30.000 39.974 49.952 59.929 69.905 79.875
156	Georgetown, DE	Dana	10.266 20.025 30.000 39.988 49.957 59.912 69.862 79.802
156	NAVOBSY	Dana	10.343 20.026 30.001 39.999 49.986 59.964 69.936 79.899
149	Toms River, NJ	Nantucket	10.513 20.163 30.001 39.907 49.841 59.792 69.758 79.740
149	NAVOBSY	Nantucket	10.456 20.150 30.001 39.909 49.845 59.795 69.756 79.728
170	Grottoes, VA	Nantucket	10.202 20.042 30.001 39.987 49.974 59.961 69.951 79.948
170	NAVOBSY	Nantucket	10.442 20.139 30.001 39.922 49.869 59.831 69.806 79.792
168	Bluefield, WV	Nantucket	9.788 20.085 30.001 39.852 49.767 59.736 69.720 79.690
168	NAVOBSY	Nantucket	10.412 20.170 30.001 39.901 49.846 59.813 69.792 79.778

### TIME OF ARRIVAL

Having determined both  $I(t-t_0)$  and  $Q(t-t_0)$ , Eq. (2) describes the loran signal as observed. The zero crossings listed in Table 5 were computed from this equation under the assumption that  $t_0$  equals zero. Each block of recorded data contained the manual input data, the voltage samples taken on seven pulses, and the UTC time at which the first sample on the first pulse in the block was taken. This UTC time, together with the zero crossing times computable from Eq. (2), make it possible to determine the TOA of any zero crossing in the pulse. None of these zero crossing times is the TOA of the phase since this notion applies to the 100-kHz carrier, and 100 kHz is not observable within the transmitted pulses. Furthermore, Eq. (2) cannot be solved for phase TOA of 100 kHz as long as cosine modulation is present. Consequently, we have had to abandon phase TOA as a meaningful measurement parameter. Instead, we have adopted the notion of "cycle" TOA; more specifically, we have adopted the "standard" TOA, that is, the TOA of the zero crossing at the end of the third cycle within the pulse.

Similar difficulties surround the definition of group TOA. In the past, group TOA has been accounted for by a combination of two parameters: the standard third-cycle TOA and ECD. ECD has been defined as the time between a specified fixed point on the pulse envelope and a specified zero crossing of the 100-kHz carrier. ECD is intended to be a measure of the position of the pulse on the carrier as would be the case if the pulse were described by the following classical formula:

$$V(t) = \left( \frac{t - ECD}{TP} \right)^K e^{-K \left( 1 - \frac{t - ECD}{TP} \right)} \sin \omega t, \quad (3)$$

where  $t$  is time referenced to the start of the pulse when ECD is zero,  
 $TP$  is the time of the peak of the pulse, usually assumed to be 65  $\mu$ s, and  
 $K$  is a constant usually assumed to be 2.

To measure ECD in a receiver, envelope tracking circuitry is used that tracks a point on the envelope defined as the tag point. This circuitry is usually adjusted initially such that the tag point is located at 30  $\mu$ s when  $t$  is 30  $\mu$ s and ECD is zero in Eq. (3). Then the difference between the envelope TOA and the standard third-cycle TOA is ECD.

Referring now to Eq. (2), it is obvious that ECD so defined defies interpretation when applied to a real pulse. A disturbing component of ECD is the difference between the TOA's of the standard third-cycle zero crossing with and without cosine modulation.

To overcome this difficulty, we have tagged the envelope differently and named a new parameter, ECM, for envelope-to-cycle measure to avoid confusion with ECD.

#### CORRECTION FUNCTION

The desired correction function, as mentioned in Section 3, is the relation of SPF to ECD. SPF has been defined in various ways. One of the classical definitions is the difference between a TOA of a 100-kHz zero crossing at the speed of light in a vacuum and the TOA at its actual propagation speed in the medium associated with the loran groundwave. As with ECD, the presence of cosine modulation makes this definition inapplicable. Consequently, we have defined a new secondary phase measure (SPM) as follows:

$$SPM = (D/C) - T_3, \quad (4)$$

where  $D$  is the distance over which the loran pulse propagates,  
 $C$  is the vacuum speed of light, and  
 $T_3$  is the TOA of the zero crossing at the end of the third cycle.

To avoid placing stringent control over envelope shape at the transmitter, we chose to examine the propagation effects over the distances between the field sites and NAVOBSY. Therefore, the  $D$  and  $T_3$  of Eq. (3) must be so interpreted, and SPM is then interpreted as the change in SPM that takes place between NAVOBSY and the field site. The values of  $D$  and SPM that apply to the test are shown in Table 6.

The change in ECM that occurs over the propagation path is best described by reference to Figs. 22 through 25. These figures show the leading edge of the pulse envelope under the constraints that the pulse envelopes are normalized to the same peak voltage and the standard third-cycle zero crossings are all aligned at  $30 \mu\text{s}$  as in Table 5. The adjustments in the time reference in Eq. (2) that are necessary to accomplish this alignment were compensated by adjustments of  $T_3$ . The change in ECM is computed by determining the difference in field site and NAVOBSY envelope voltage at  $30 \mu\text{s}$  and converting this voltage to time using the average slope of the envelopes evaluated at  $30 \mu\text{s}$ . These changes in ECM are shown in Table 6.

Figure 26 is a plot of the change in SPM versus the change in ECM. This figure is a representation of the correction function for the SPF that had been anticipated. Obviously, it leaves something to be desired.

Table 6  
 Values of SPM and ECM Plotted in Fig. 26

1975 Day No.	Field Site	Transmitting Station	NAVOBSY to Field Site (m)	SPM ( $\mu$ s)	ECM ( $\mu$ s)
177	Wilmington, NC	Carolina Beach	-520 672	-3.600	-1.653
			-520 672	-3.600	-1.656
			-520 672	-3.600	-1.673
175	Emporia, VA	Carolina Beach	-250 900	-1.490	-0.772
			-250 900	-1.491	-0.829
			-250 900	-1.489	-0.831
183	Towanda, PA	Carolina Beach	323 487	2.713	-0.223
			323 487	2.736	-0.049
			323 487	2.720	-0.032
181	Dexter, NY	Carolina Beach	569 702	3.894	-0.105
			569 702	3.901	-0.355
			569 702	3.904	-0.369
163	Danville, IN	Dana	-817 137	-5.562	-5.301
			-817 137	-5.555	-5.367
			-817 137	-5.558	-5.346
161	Marietta, OH	Dana	-376 178	-3.172	-2.272
			-376 178	-3.165	-2.120
			-376 178	-3.165	-2.353
156	Georgetown, DE	Dana	150 434	0.677	-3.759
			150 434	0.680	-5.212
			150 434	0.679	-7.223
149	Toms River, NJ	Nantucket	-273 230	-2.092	-1.053
			-273 230	-2.074	-1.014
			-273 230	-2.084	-1.100
170	Grottoes, VA	Nantucket	170 013	1.891	-0.689
			170 013	1.896	-0.985
			170 013	1.914	-1.256
168	Bluefield, WV	Nantucket	405 849	3.019	2.272
			405 849	3.023	1.897
			405 849	3.031	1.879
154	NAVOBSY	Carolina Beach	0	0.026	-0.010
			0	0.037	0.149
			0	0.044	0.153
188	NAVOBSY	Carolina Beach	0	0.046	0.053
			0	0.048	0.048

LORAN-C SIGNAL VOLTAGE PLOTTED AGAINST TIME IN MICROSECONDS  
1975 DAY NO.: 177  
FIELD SITE: WILMINGTON, NC STATION: CAROLINA BEACH XMTR: 19 DATA SEGMENT: ALL

. ↔ NAVOBSY + ↔ FIELD SITE

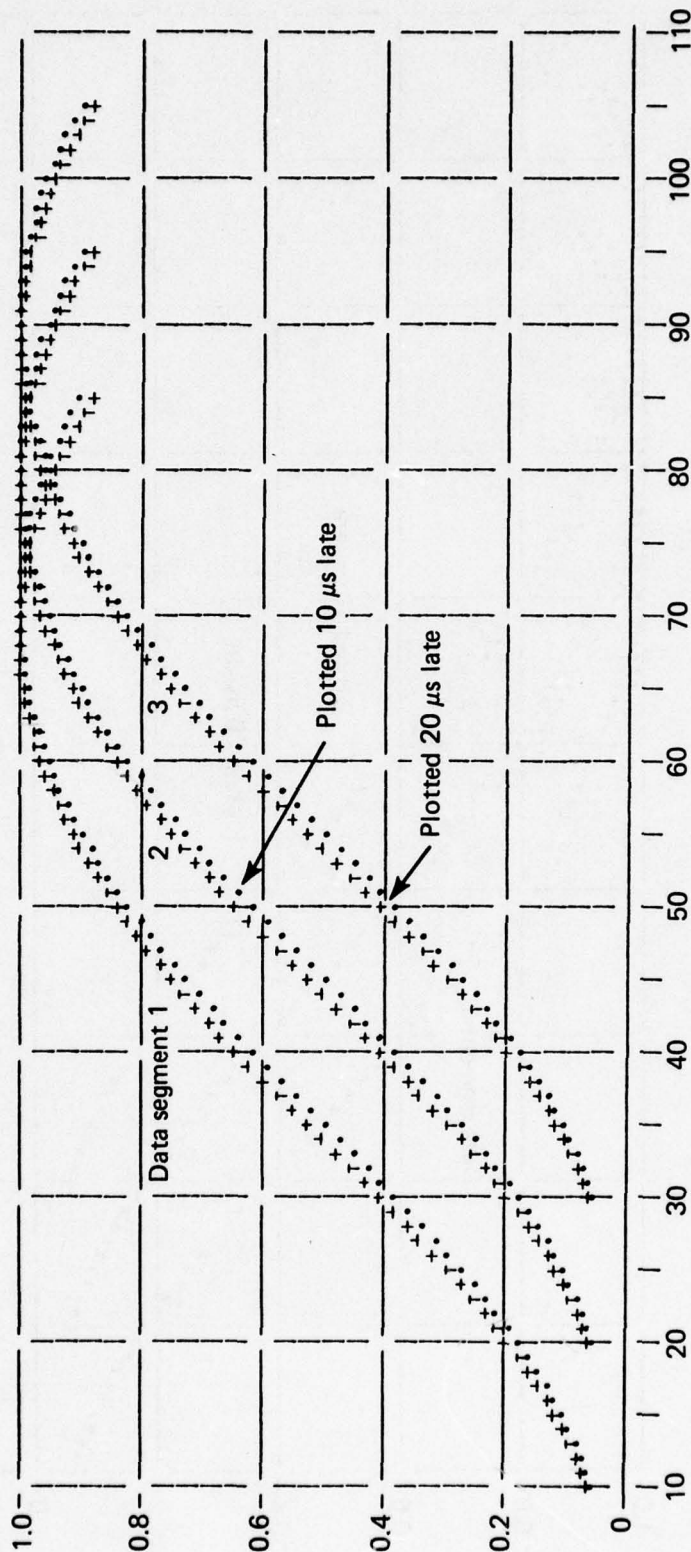


Fig. 22 Locations of Leading Edges of Pulses with Standard Zero Crossings Aligned at 30 μs, Wilmington, NC, and NAVOBSY

403A-V-C SIGNAL VOLTAGE PLOTTED AGAINST TIME IN MICROSECONDS  
 FIELD SITE: DEXTER, NY STATION: CAROLINA BEACH XMTR: 19 DATA SEGMENT: ALL  
 1975 DAY NO.: 181

. ↔NAVOBSY + ↔FIELD SITE

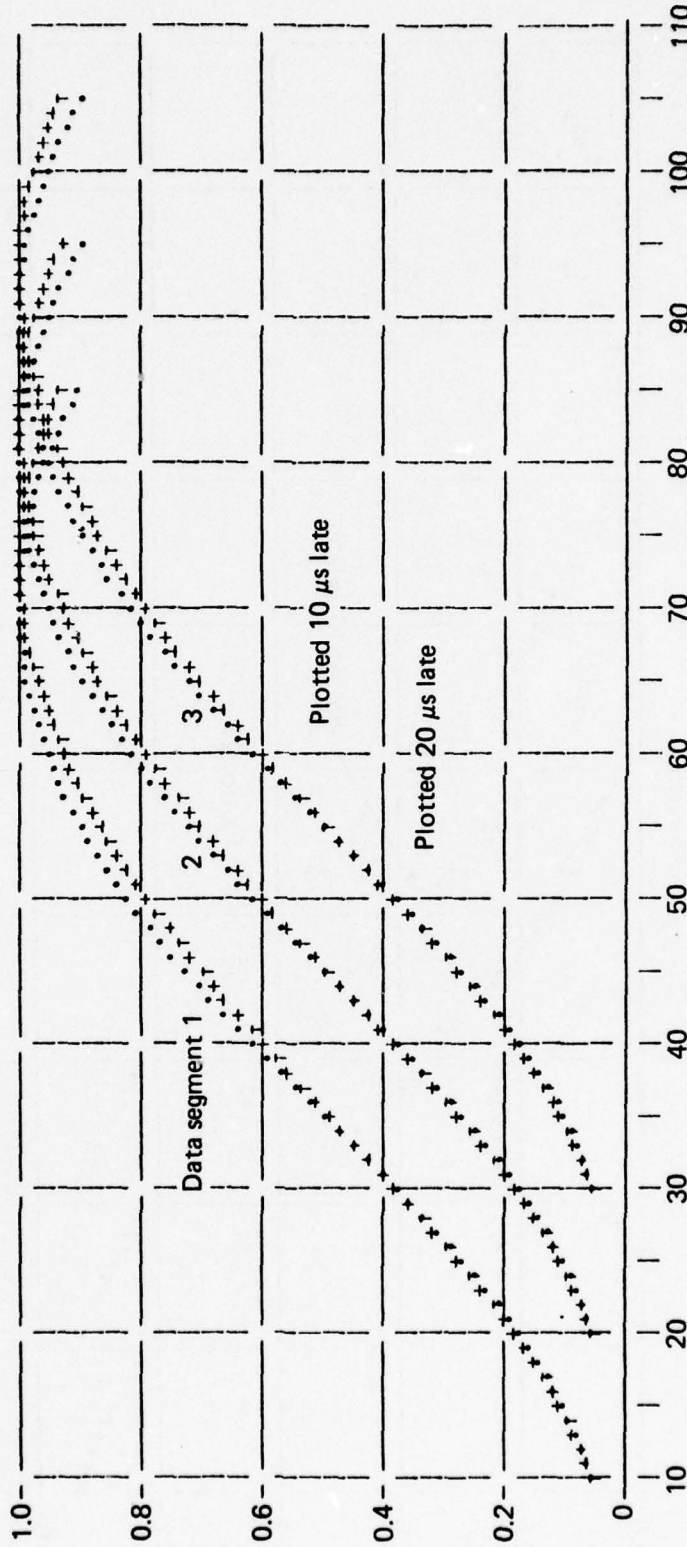


Fig. 23 Locations of Leading Edges of Pulses with Standard Zero Crossings Aligned at 30 μs, Dexter, NY, and NAVOBSY

LORAN-C SIGNAL VOLTAGE PLOTTED AGAINST TIME IN MICROSECONDS  
 FIELD SITE: DANVILLE, IN STATION: DANA XMTTR: 19 DATA SEGMENT: ALL

. ↔NAVBOBSY + ↔FIELD SITE

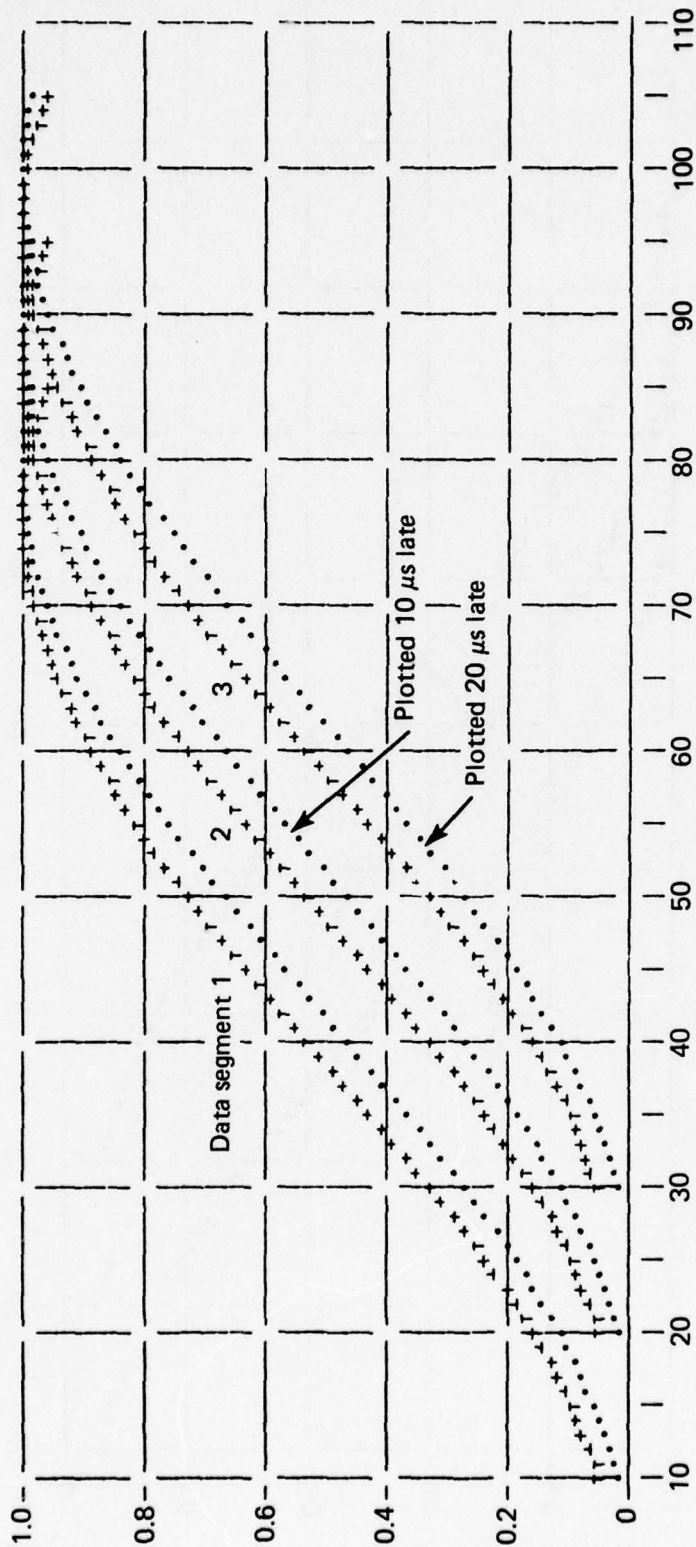


Fig. 24 Locations of Leading Edges of Pulses with Standard Zero Crossings Aligned at 30 μs, Danville, IN, and NAVBOBSY

LORAN-C SIGNAL VOLTAGE PLOTTED AGAINST TIME IN MICROSECONDS  
 1975 DAY NO.: 149  
 FIELD SITE: TOMS RIVER, NJ STATION: NANTUCKET XMT: 23 DATA SEGMENT: ALL

. ↔NAVOBSY + ↔FIELD SITE

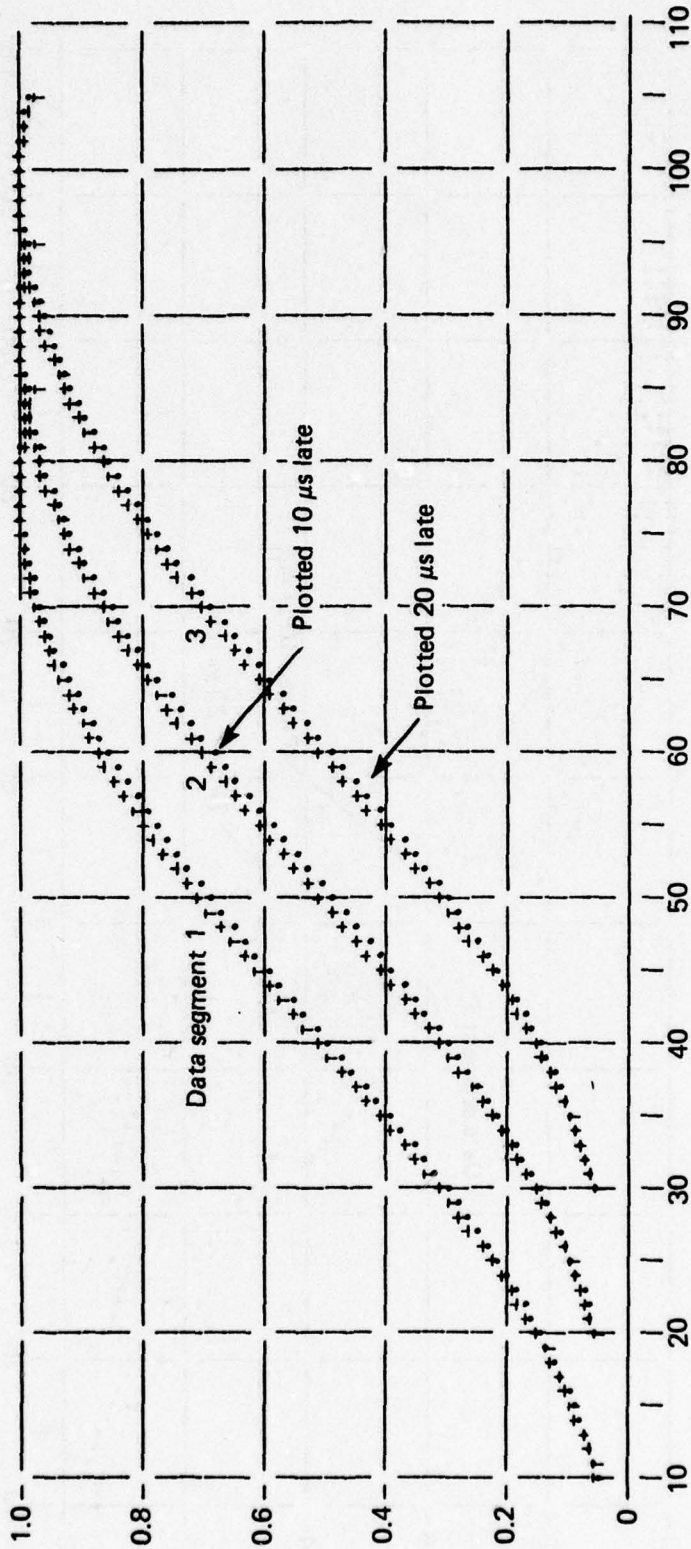
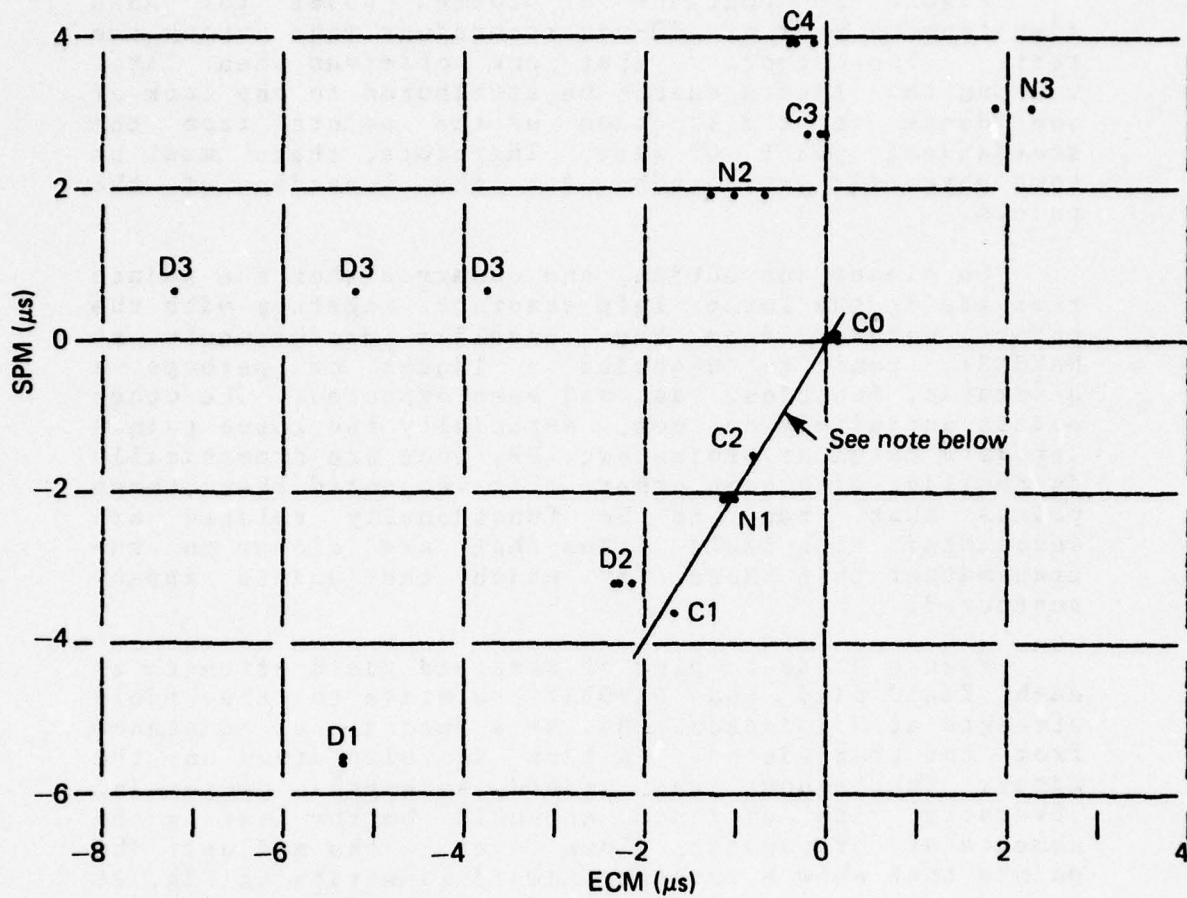


Fig. 25 Locations of Leading Edges of Pulses with Standard Zero Crossings Aligned at 30 μs, Toms River, NJ, and NAVOBSY



Note: The straight line is drawn through points for which both the field site and NAVOBSY are close to the inverse distance line in Fig. 27.

Fig. 26 The Relationship Between SPM and ECM

## 6. DISCUSSION OF RESULTS

Figure 26 contains a plotted point for each simultaneous pair of 20-min recordings made during the test. The disorder that one observes when first viewing this figure cannot be attributed to any lack of confidence in the location of the points from the statistical point of view. Therefore, there must be some physical explanation for the location of the points.

On closer inspection, one observes that the points that lie in the lower left quadrant, together with the points derived from the baseline measurements at NAVOBSY, tend to describe a linear, or perhaps a quadratic, function, as had been expected. The other points definitely do not, especially the three points for data taken at Georgetown, DE, that are dramatically in conflict with each other. It was noted that those points that tend to be functionally related are associated with field sites that are closer to the transmitter than those for which the points appear scattered.

Figure 27 is a plot of observed field strength at each field site and NAVOBSY relative to the field strength at Wilmington, NC, as a function of distance from the transmitter. A line is also drawn on the figure that shows the field strength decreasing inversely with distance, as would be the case in the absence of propagation loss due to the medium. The points that show a tendency toward linearity in Fig. 26 are very close to the inverse distance line in Fig. 27, and those that scatter in Fig. 26 are far off the inverse distance line. This tends to indicate that the pulses associated with the scattered points on Fig. 26 have been significantly influenced by the medium in a way that had not been expected.

This observation is borne out by Figs. 14 and 15 and Figs. 18 and 19. Note that in Fig. 14 very little change in the cosine modulation has occurred between Wilmington, NC, and NAVOBSY, whereas substantial change occurs between NAVOBSY and Dexter, NY. In Fig. 18, the change in envelope shape is insignificant between Wilmington and NAVOBSY, but the envelope at Dexter is significantly stretched relative to that at NAVOBSY. This is another aspect of the problem of associating a simple measure, such as ECD, with propagation effects on the radiated pulses.

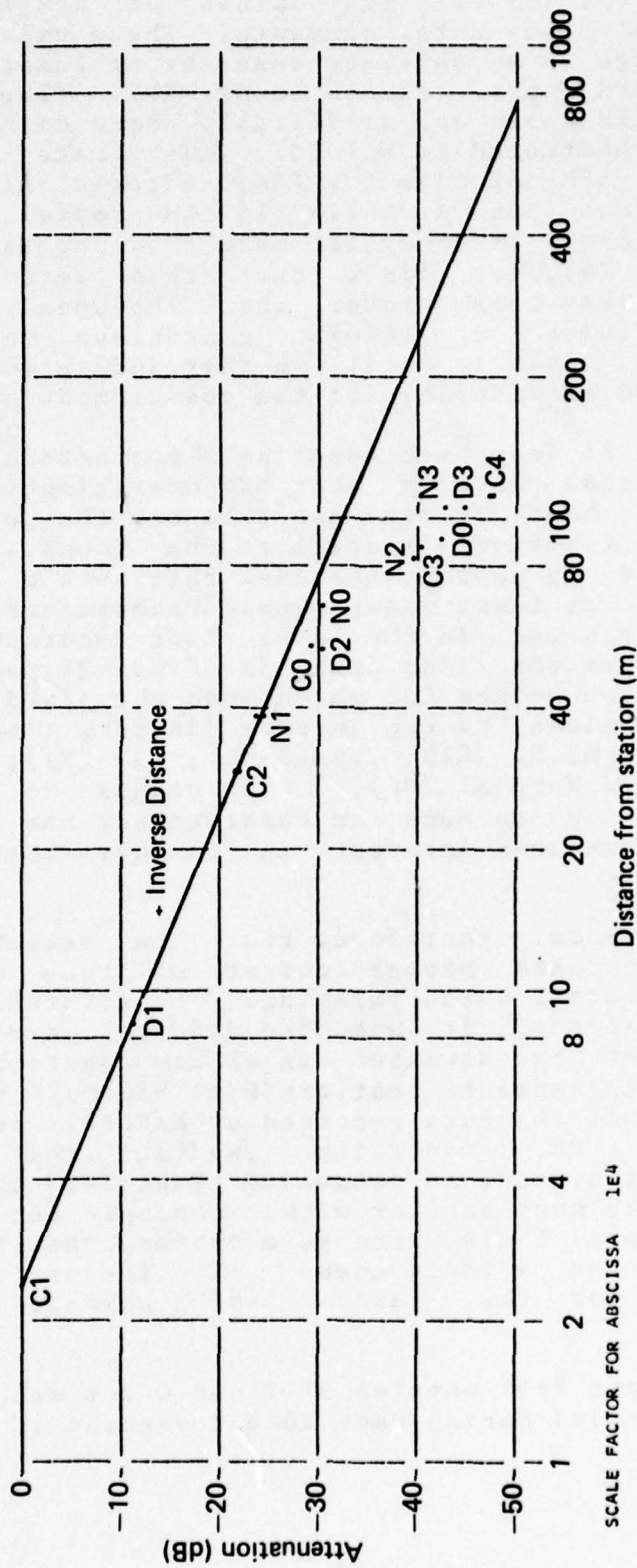


Fig. 27 Attenuation of the Signal Relative to the Field Strength of Carolina Beach Observed at Wilmington, NC

Table 6 lists all the values of SPM determined from each of the data segments. These values of SPM are too large in an absolute sense by at least a factor of two if SPM were assumed to be SPF. (The negative values of SPM shown are artificial. Both distance and time were referenced to NAVOBSY, which makes distance, time, and SPM negative for field sites closer to the loran stations than NAVOBSY.) If the propagation speed of the standard third-cycle zero crossing is computed using Eq. (4), one finds that this zero crossing propagates very much slower than the speed commonly associated with a 100-kHz continuous wave (CW) groundwave. This is still another indication of the complication attributable to the cosine modulation.

Figure 26 does not describe a correction function for propagation effects that has operational utility. On the other hand, it does not rule out the possibility that such a function is still to be found. In fact, Fig. 26 tends to support the idea that such a function should exist at least under some circumstances, to wit, the points plotted in the lower left quadrant. Note that the straight line drawn in Fig. 26 passes very close to those points for which both the field site and NAVOBSY lie close to the inverse distance line of Fig. 27: Wilmington, NC (C1); Toms River, NJ (N1); Emporia, VA (C2); and NAVOBSY (C0). Four points do not lend high confidence to such an observation, but they do stimulate continued interest in further testing and analysis.

It appears, therefore, that the search for a formula that takes proper account of group and phase velocity is still worth pursuing. As a first step in further analysis, it was decided to explore the influence of the unwanted signal components contained in those data segments that exhibit bimodal histogram contours. All the data recorded at NAVOBSY during the Georgetown, DE, recording exhibit the bimodal characteristic, and, as shown in Fig. 26, these data result in the most scatter within a single set of three data segments. These data were chosen, therefore, for exploring the effectiveness of frequency domain filtering for the removal of unwanted signal components.

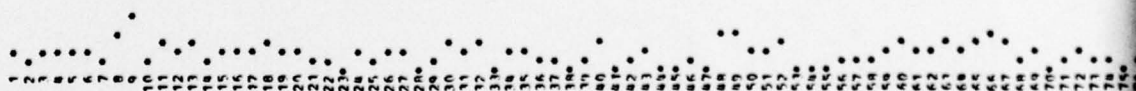
The first 8192 samples of I and Q for each pair of samples recorded during each 20-min segment at NAVOBSY

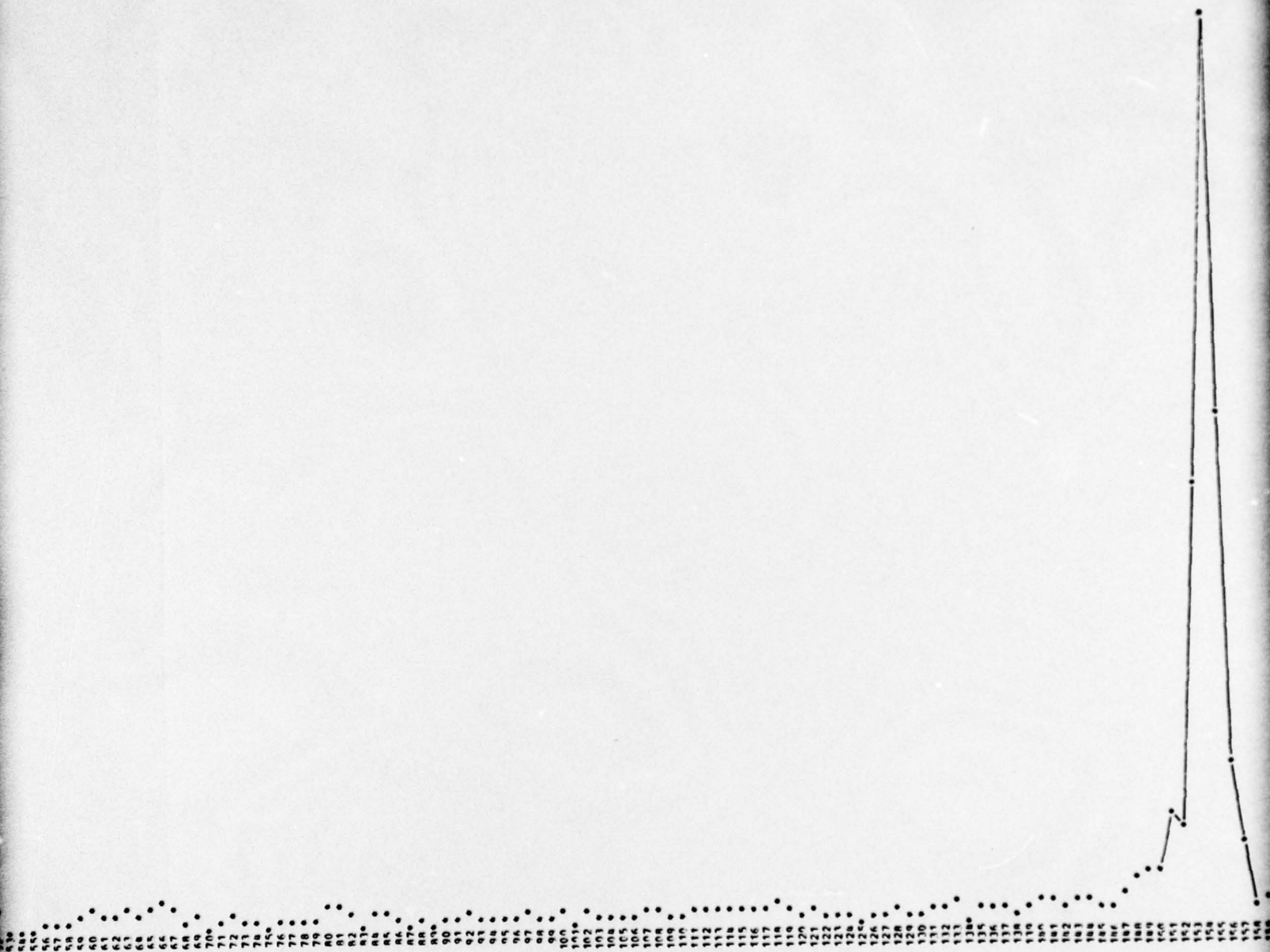
and Georgetown were subjected to a Fourier analysis that identified frequency components in the data that had the potential of interference with the Loran spectrum. These frequencies were identified by observing those Fourier coefficients that contain a significant fraction of the noise power. Figure 28 is an example of plots used for identifying interference. The effect of these unwanted frequencies was then removed by substituting zero for the unwanted coefficients. The inverse transform was then performed, which produced an estimate of the 8192-point data set that would have been observed in the absence of the unwanted signals.

Figures 29 and 30 are histograms of data recorded at Georgetown before and after frequency filtering. Note that the centrally located cluster of points exhibits slightly elliptical contours in Fig. 29, and, in Fig. 30, the cluster is reduced in size and is reasonably circular. Figures 31 and 32 are histograms of the data recorded simultaneously at NAVOBSY. Note, in this case, that the cluster of points in Fig. 31 is very elliptical, and, after filtering, the ellipticity and size of the cluster in Fig. 32 are reduced. A comparison of the means of the filtered data with the means of the first-stage edited data indicates that frequency domain filtering caused changes in their values that might be large enough to have significant influence on the results of subsequent analysis. Whether or not frequency domain filtering removes the cause of the scatter observed in Fig. 26 has not been determined, because the rather significant effort to do so had not been foreseen and included in the original program plan.

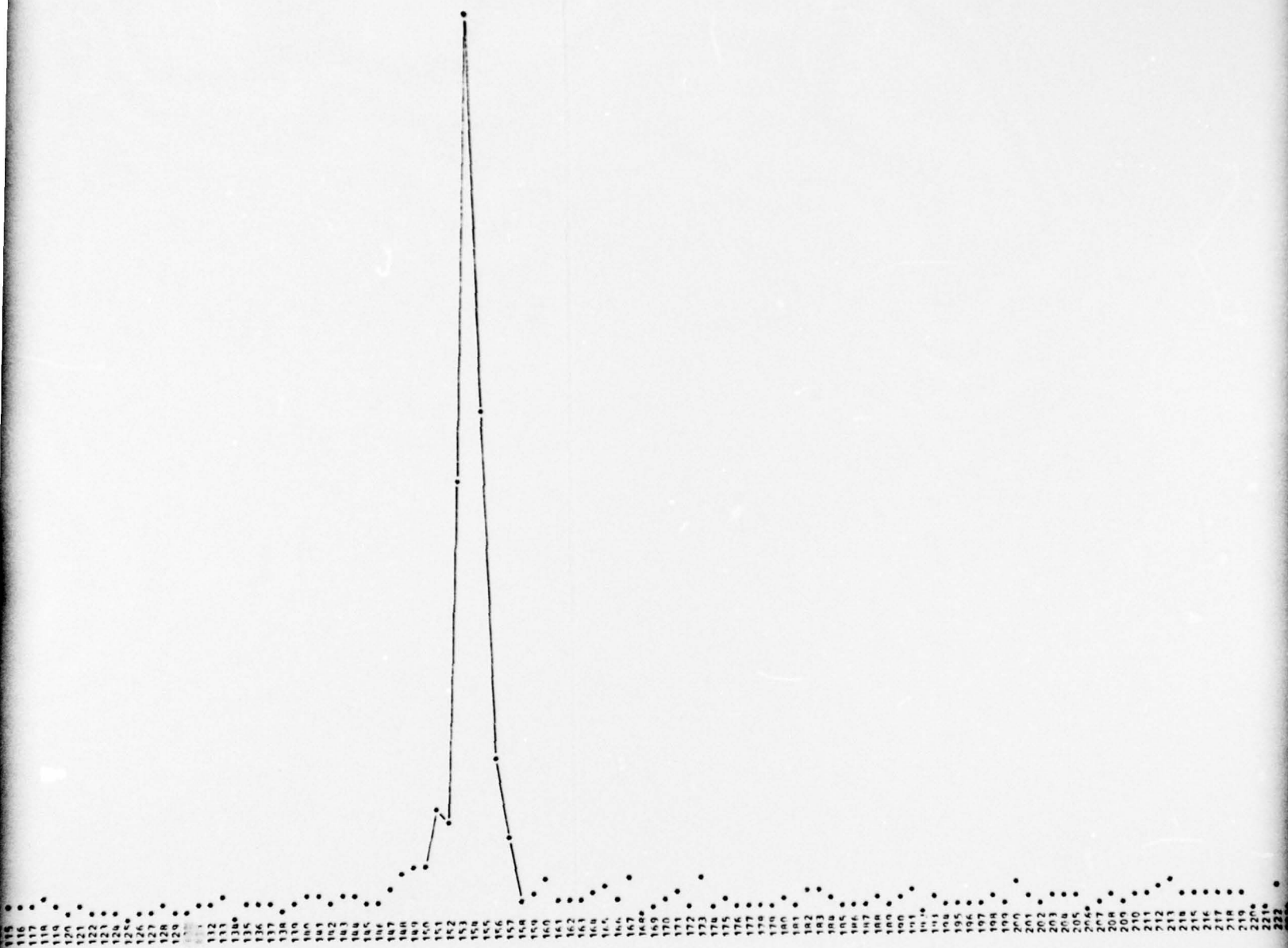
As a final observation, it should be pointed out that theoretical predictions of the arrival time of zero crossings in current Loran-C pulses are limited in accuracy if the cosine component of the pulse is not taken into account.

TOTAL DC POWER IN  $\theta = 0.0314$   
Power





Frequency



Frequency

Fig. 28 Power Spect

Preced

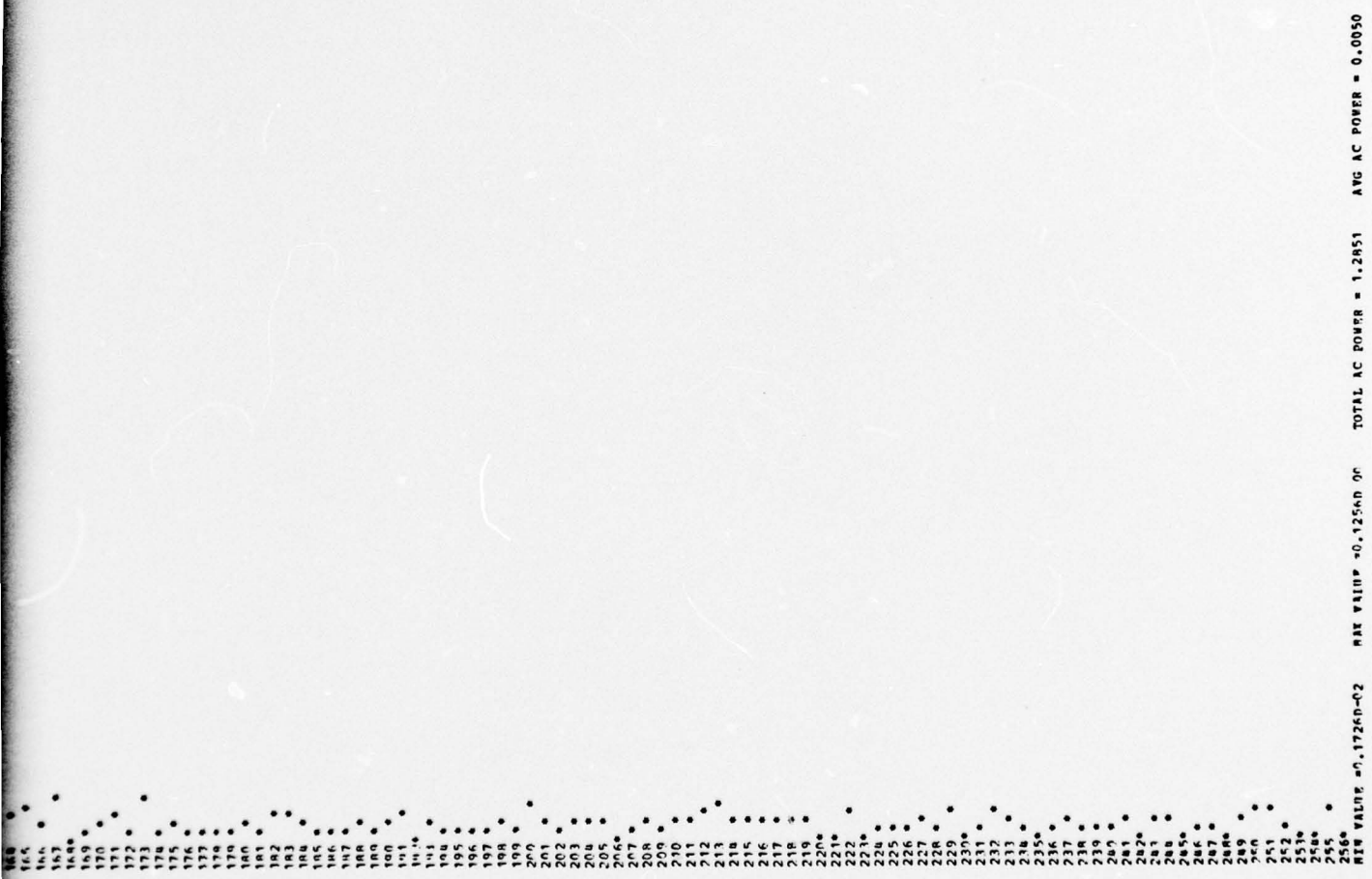


Fig. 28 Power Spectral Density Showing Interference at 179 kHz

Preceding page blank

T11-T12 HISTOGRAM

	0	0	0	0	0	0	1	0	0	3	0	1	0	0	0	0	0	1	0	0	T11
	0	0	0	0	0	1	1	0	0	1	2	0	0	1	0	0	0	0	0	0	6
	0	0	0	0	0	1	1	0	0	1	2	0	0	1	0	0	0	0	0	0	6
	1	0	0	0	0	2	1	0	0	1	2	0	0	1	0	0	0	0	0	1	9
	0	1	0	0	0	0	0	1	1	0	1	2	1	0	0	2	0	0	0	0	9
	0	0	0	1	2	1	2	3	2	0	0	0	1	2	2	0	0	0	0	0	16
	0	0	0	1	1	2	3	4	4	1	5	2	1	0	1	0	1	0	0	0	29
	0	0	0	0	2	0	4	11	12	12	7	4	3	3	1	2	0	1	0	1	65
	0	0	1	2	4	4	6	13	46	55	35	15	10	2	2	0	0	2	0	0	199
Quadrature	0	0	2	1	1	4	15	41	330	417	141	34	26	3	3	2	0	3	1	0	1024
	0	0	1	3	4	6	17	58	433	1243	444	130	33	11	5	3	4	0	0	1	2612
	0	1	1	1	2	1	11	27	152	764	1310	425	51	11	6	4	1	2	0	0	2770
	0	0	1	1	1	2	4	17	47	110	443	304	48	9	4	4	1	1	0	0	1025
	0	1	0	0	1	1	3	10	11	42	52	41	17	8	3	2	2	0	0	0	194
	0	0	0	1	0	2	2	1	9	9	12	15	8	3	3	1	1	1	0	0	68
	0	0	0	2	0	0	1	4	4	4	5	5	7	4	1	2	0	1	1	0	41
	0	0	0	0	0	1	0	0	0	3	0	0	2	1	3	0	0	0	0	0	10
	0	0	0	0	1	0	1	0	1	1	0	2	0	1	1	1	0	0	0	0	9
	0	0	0	0	0	0	1	1	2	0	0	0	0	0	1	0	0	0	0	1	6
	0	0	0	0	0	0	0	0	1	1	0	0	0	0	1	0	0	1	0	0	4
	0	0	0	0	0	0	1	0	0	1	1	0	1	0	0	0	1	1	0	0	6

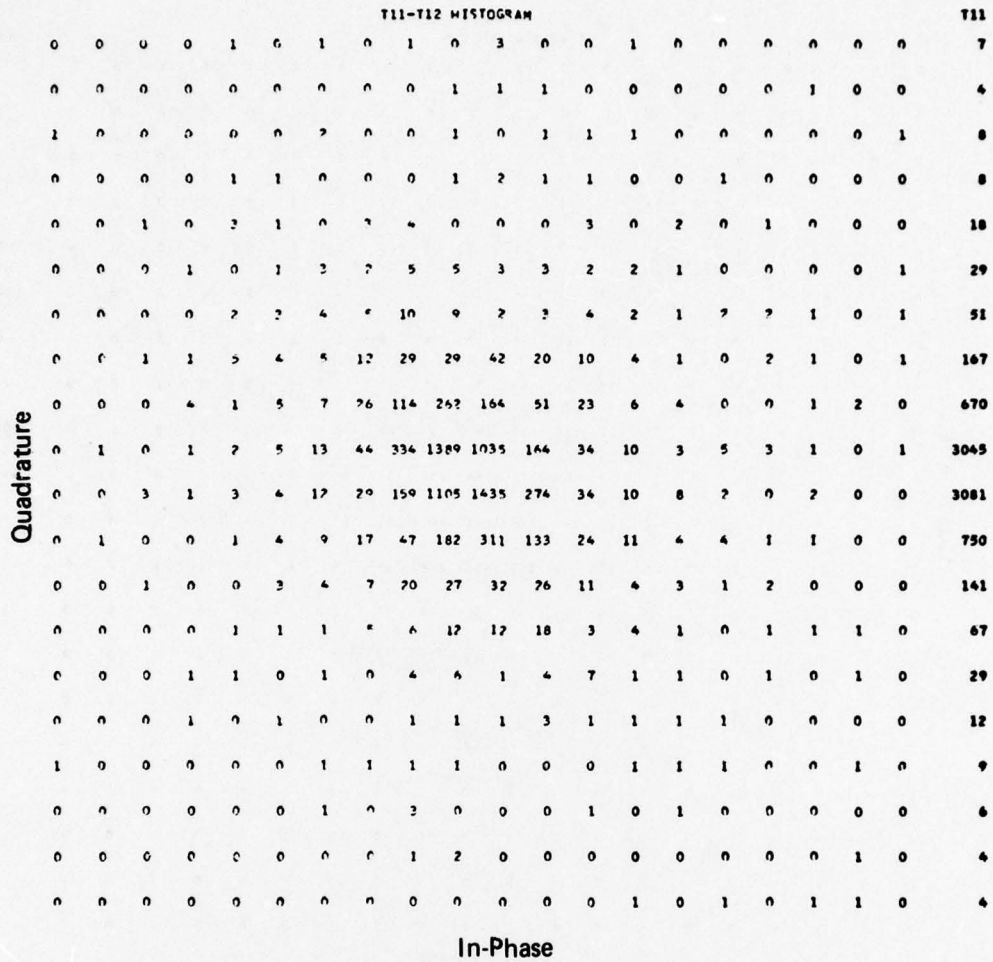
In-Phase

T12 DISTRIBUTION  
 1 3 6 13 19 33 70 100 1057 2691 2676 983 210 61 38 25 11 15 2 4

TOTAL NO. PAIRS = 8192  
 T11-T12 EDIT SIGMA = 0.6249  
 FITTING LEVEL = 6 SIGMA  
 T11 EDIT PAIRS = 35  
 T12 EDIT PAIRS = 37  
 T11-T12 EDIT PAIRS = 12  
 T11 AVERAGE = 0.1042  
 T12 AVERAGE = 0.9175

Fig. 29 Histogram of First-Stage Edited Data Taken at Georgetown, DE

Preceding page blank



T12 DISTRIBUTION  
 2 2 6 10 21 37 64 151 739 3033 3044 702 159 59 32 18 13 10 7 5

TOTAL NO. PAIRS = 8192  
 T11,12 EDIT SIGMA = 0.6249  
 EDITING LEVEL = 6 SIGMA  
 T11 EDIT PAIRS = 37  
 T12 EDIT PAIRS = 35  
 T11,12 EDIT PAIRS = 10  
 T11 AVERAGE = 0.1044  
 T12 AVERAGE = 0.9165

Fig. 30 Histogram of First-Stage Edited Data Taken at Georgetown, DE, after Frequency Filtering

T11-T12 HISTOGRAM

		T11-T12 HISTOGRAM																T11			
	0	0	0	0	0	0	0	0	0	0	1	0	0	0	0	0	1	0	0	0	2
	0	0	0	0	1	0	0	1	1	1	0	0	1	0	0	0	0	0	0	0	5
	0	0	0	0	0	1	0	0	0	1	0	0	1	1	1	0	0	0	0	5	
	0	0	0	0	0	1	1	0	0	0	1	1	0	1	1	0	0	0	0	8	
	0	0	1	1	1	0	2	0	0	0	1	0	1	1	1	0	0	0	0	11	
	0	2	0	1	1	4	1	5	6	4	5	5	2	2	1	0	0	0	0	60	
	0	0	0	0	3	1	4	8	18	17	12	4	6	4	2	0	0	0	2	81	
	0	0	0	3	2	9	3	33	86	62	26	19	6	7	6	0	3	1	0	266	
Quadrature	0	1	1	0	3	5	18	82	640	499	118	37	13	12	0	0	1	1	1	1819	
	0	0	1	1	5	5	9	66	462	1078	463	98	29	15	5	4	0	3	1	2285	
	0	2	0	1	0	9	13	27	96	503	1076	506	66	11	8	1	2	0	0	2322	
	1	0	1	0	2	2	8	19	27	96	508	574	76	14	5	2	1	0	3	1339	
	0	1	1	0	1	0	4	11	17	24	54	74	32	10	1	6	0	0	0	280	
	0	1	0	1	0	2	2	2	4	9	17	15	10	1	2	4	0	0	0	70	
	0	0	0	0	0	1	2	0	5	7	5	6	4	2	1	2	0	0	0	35	
	0	0	0	1	0	0	1	3	3	3	5	4	0	3	0	2	0	0	0	25	
	0	1	0	0	0	0	0	1	1	1	1	0	2	2	2	0	0	0	0	11	
	0	0	0	0	1	0	1	1	2	0	1	0	0	0	0	0	0	0	0	6	
	0	0	0	0	1	0	1	0	1	0	0	0	0	0	0	0	0	0	1	5	
	0	0	1	0	1	0	0	0	0	0	0	0	0	0	0	0	0	0	0	2	

In-Phase

T12 DISTRIBUTION

1	7	6	9	22	40	70	259	1369	2295	2292	1349	248	86	36	22	8	5	8	5
---	---	---	---	----	----	----	-----	------	------	------	------	-----	----	----	----	---	---	---	---

TOTAL NO. PAIRS = 8192  
 T11,12 EDIT SIGMA = 0.7757  
 EDITING LEVEL = 6 SIGMA  
 T11 EDIT PAIRS = 22  
 T12 EDIT PAIRS = 24  
 T11,12 EDIT PAIRS = 9  
 T11 AVERAGE = 0.0395  
 T12 AVERAGE = 1.2246

**Fig. 31 Histogram of First-Stage Edited Data Taken at NAVOBSY During Recording at Georgetown, DE**



## 7. CONCLUDING REMARKS

The problem that we set out to solve was far more complicated than we had expected. The principal reason for this was the presence of significant cosine modulation in the signals radiated from the Carolina Beach, Nantucket, and Dana Loran-C Stations. The presence of this modulation makes it impossible to observe the carrier phase TOA and the ECD with respect to it.

Further analysis of the recorded data shows promise of discovering meaningful measurement parameters that may make it possible to account for group and phase propagation velocity even in the presence of cosine modulation. As a first step in further analysis, it appears that all the data should be subjected uniformly to frequency domain filtering (as was tried on the Georgetown data). The next step should be a Fourier analysis performed on the Loran-C pulses observed at all sites so that propagation effects on the individual lines of the spectrum can be understood. It is believed that such an analysis would disclose the relationship between group and phase propagation velocity that pertains to the propagation of Loran-C pulses as actually radiated. As a last step, operationally useful measurement parameters might be identified and associated with an appropriate equation relating them to the distance between the transmitter and the point of observation.

As mentioned earlier, there is some evidence in Fig. 26 that the anticipated function relating SPF to ECD tends to be exhibited by the points plotted for distances less than those at which propagation losses due to the medium become significant. The precise definition of this function is clouded by the presence of cosine modulation. Whether or not the definition would be clear in the absence of cosine modulation cannot be determined from the data taken. Additional Loran-C data taken with the fixed site moved to the field sites nearest the transmitter would be helpful in resolving this question. Should loran transmitters become available that produce only amplitude modulation on the carrier, it would be very desirable to gather additional data to explore further the definition of a correction function that is specifically applicable to AM modulated signals. We expect that such a function

should be much simpler than one that is applicable in the presence of both sine and cosine modulation.

We would be remiss not to highlight the high quality of the radiated Loran-C signals from the statistical point of view. Loran pulses that survive time domain editing of the signals are very accurate estimates of noise-free pulses. Dexter, NY, is 1114 km from Carolina Beach. Georgetown, DE, is 1054 km from Dana, and Bluefield, WV, is 1063 km from Nantucket. Nevertheless, the S/N ratio of edited data for single pulses (i.e., no integration) at Dexter was 23 dB; at Georgetown, 8 dB; and at Bluefield, 11 dB. These values apply well within 1 dB to the standard tracking point at the end of the third cycle. If a receiver had a time constant that produced the equivalent of integrating 400 of these edited pulses, the standard deviation of the output of the tracking loop would be 6 ns at Dexter, 32 ns at Georgetown, and 22 ns at Bluefield. Assuming that the statistics associated with the second through eighth pulses in a group are not significantly different from the statistics of the first pulse, such a receiver would have a time constant of about 5 s.

As a final comment on the quality of the loran signals, the data taken at Wilmington, NC, and at Danville, IN, were taken within 24 km and 86 km of the respective transmitters. At these ranges, the field strength of the signal is so large at the receiving antenna that noise at the antenna that survives time domain editing is negligible by comparison. The S/N ratio observed at Wilmington and Danville after editing, therefore, can be attributed almost exclusively to transmitter jitter and receiver self-noise. In both locations, the S/N ratio was 34 dB at the track point (again, no integration). This S/N ratio converts to a TOA standard deviation of 32 ns. Since the receiver self-noise contributes about 16 ns, it can be inferred that the transmitter jitter contributes about 27 ns to the per-pulse standard deviation.

## 8. RECOMMENDATIONS

The original goal of this experiment is still worth pursuing. It is recommended that analysis of the existing data be continued at least until propagation effects on group and phase velocity associated with loran signals are understood. Contingent on this understanding, it is recommended that measurement parameters be identified that have operational utility in determining the distance over which the loran signal propagates.

It is also recommended that additional data be taken on the Dana and Carolina Beach ray paths with the fixed site moved to the field site closest to the transmitter. This would determine the distance to which a linear correction function might be applicable.

Consideration should be given to repeating the experiment when loran transmitters become available that have the capability of transmitting pure AM modulated signals.

## 9. ACKNOWLEDGMENTS

The authors wish to express their appreciation to the many individuals who participated in the experiment. They brought to bear on the problem a wide variety of technologies in such an expert manner as to make one remember our past associations with great pleasure. The successful completion of the test was undoubtedly attributable to their assistance. Specific contributions of our associates are acknowledged in Volumes B, C, and D.

10. REFERENCES

1. Anon., "Loran-C System Description," Radionavigation Journal, Wild Goose Association, 1975.
2. H. Sommerfeld, "About the Propagation of Light in Dispersive Media," Ann. Physik, 1914.
3. L. Brillouin, "About the Propagation of Light in Dispersive Media," Ann. Physik, 1914.
4. L. Brillouin, Wave Propagation and Group Velocity, Academic Press, 1960.
5. J. A. Stratton, Electromagnetic Theory, McGraw-Hill, 1941.
6. V. Schwab, "Measurement Definitions and Algorithms for Transit Integral Doppler and Ranging Navigation Systems," APL/JHU S3-R-023, January 1974.
7. V. Schwab and E. F. Prozeller, "Single-Frequency Refraction-Free Satellite Navigation," APL/JHU TG 1221, January 1974.
8. Anon., "Minutes of LORIG Meeting of 30-31 January 1973," USAF, ESD, Loran System Program Office.
9. USAF Loran System Program Office, "Envelope/Cycle Phase-Shift Study," USAF ltr. ESD/DCL, 30 March 1973.
10. K.M. Evenson et al., "Speed of Light from Direct Frequency and Wavelength Measurements of the Methane-Stabilized Laser," Physical Review Letters, 6 November 1972.
11. Anon., "Report of the DoD Geociever Test Program," DoD Defense Mapping Agency Report 001, July 1972.
12. Anon., "Specification for Loran-C Monitor Receiver," U.S. Coast Guard Report EEE-4-72, 1972.
13. Anon., "Minimum Performance Standards--Airborne Loran-C and Loran-C Receiving Equipment," RTCA Document DO-159, 17 October 1975.